

# Detection of Risk Predictors of COVID-19 Mortality with Classifier Machine Learning Models Operated with Routine Laboratory Biomarkers

Mehmet Tahir Huyut <sup>1,\*</sup>, Andrei Velichko <sup>2</sup> and Maksim Belyaev <sup>2</sup>

<sup>1</sup> Department of Biostatistics and Medical Informatics, Faculty of Medicine, Erzincan Binali Yıldırım University, 24000, Erzincan, Turkey

<sup>2</sup> Institute of Physics and Technology, Petrozavodsk State University, 33 Lenin str., 185910, Petrozavodsk, Russia

\* Correspondence: [tahir.huyut@erzincan.edu.tr](mailto:tahir.huyut@erzincan.edu.tr)

## Abstract

Early evaluation of patients who require special care and high death expectancy in COVID-19 and effective determination of relevant biomarkers on large sample groups are important to reduce mortality. This study aimed to reveal the routine blood value predictors of COVID-19 mortality and to determine the lethal risk levels of these predictors during the disease process. The dataset of the study consists of 38 routine blood values of 2597 patients who died ( $n = 233$ ) and recovered ( $n = 2364$ ) from COVID-19 in August-December, 2021. In this study, 16 popular classifier machine learning models were operated with 34 features that it was selected statistically and their performance in classifying patient groups was examined. Histogram-based gradient boosting (HGB) model was the most successful ML classifier in detecting living and deceased COVID-19 patients (with squared F1 metrics  $F1^2 = 1$ ). The most efficient binary combinations with procalcitonin were obtained with D-dimer, ESR, D.Bil and ferritin. The HGB model operated with these couples correctly detected almost all of the patients who survived and died. (precision  $> 0.98$ , recall  $> 0.98$ ,  $F1^2 > 0.98$ ). Furthermore, in the HGB model operated with a single feature, the most efficient features were Procalcitonin ( $F1^2 = 0.96$ ) and ferritin ( $F1^2 = 0.91$ ). In addition, according to the two-threshold approach ferritin values between 376.2  $\mu\text{g/L}$  and 396.0  $\mu\text{g/L}$  ( $F1^2 = 0.91$ ) and procalcitonin values between 0.2  $\mu\text{g/L}$  and 5.2  $\mu\text{g/L}$  ( $F1^2 = 0.95$ ) were found to be fatal risk levels for COVID-19. Considering all the results, we suggest that many features combined with these features, especially procalcitonin and ferritin, operated with the HGB model, can be used to achieve very successful results in the classification of those who live and die from COVID-19. Moreover, we strongly recommend that clinicians consider the critical levels we have found for procalcitonin and ferritin properties to reduce the lethality of COVID-19 disease.

**Keywords:** COVID-19, mortality risk biomarkers, immunological tests, ferritin, procalcitonin, Histogram-based gradient boosting, classifier machine learning, artificial intelligence.

---

## 1. Introduction

The complexity of severe acute respiratory syndrome coronavirus 2 (SARS-CoV-2/COVID-19), the rapid spread of the disease, causing serious and fatal complications has focused researchers on the clinical course of the disease [1,2]. The disease has placed an unprecedented strain on healthcare systems around the world and has put medical professionals in an unknown and challenging effort to treat populations of patients with a new and deadly disease [3–5].

Although important information about the genetic structure of this new virus has been obtained [6] and data on the symptoms of the disease are shared in the medical community [7], there are still many severe cases exist. Mortality rates for this disease differ between countries [8–10] and workload in hospitals affects mortality [3,10].

While mild symptoms (fever, dry cough, shortness of breath, myalgia, fatigue, etc.) are seen in most of the patients with SARS-CoV-2 infection, it has been stated that acute respiratory distress syndrome, septic shock, bleeding, coagulation disorder and metabolic acidosis can be seen and result in death in severe cases noted that this disease can accompany multi-organ dysfunction and cause a variety of symptoms [11–15]. Onur et al. [16] and Huyut et al. [12] reported that COVID-19 disease may be asymptomatic or associated with severe ARDS thought to be due to inflammatory cytokine storm. Furthermore, Chalmers et al. [17] noted that excessive and uncontrolled release of proinflammatory cytokines may be considered the most important primary cause of death from coronavirus, as has been reported in other infections caused by pathogenic coronaviruses. However, attempts to identify and treat hyperinflammation associated with COVID-19 infection continue [18].

Many studies have indicated that male gender, advanced age, comorbidities such as chronic obstructive pulmonary disease (COPD) and diabetes mellitus, and some routine laboratory tests such as D-dimer, procalcitonin, CRP are associated with worse outcomes of the disease [4,14,19–23] stated that COVID-19 patients with severe pneumonia have decreased serum albumin and prealbumin levels and signs of deterioration in liver and kidney functions.

Most of the previous routine blood studies were aimed at identifying features that affect the diagnosis and prognosis of COVID-19 [4,22,23]. However, as the number of infected and fatal cases increases worldwide, there remains a need for detailed investigation of clinical, radiological and laboratory features, and more importantly, mortality risk factors in severe COVID-19 patients [11,24]. Zhang et al. [24] noted that there may be changes in the previously detected predictive values of mortality in severe and critical COVID-19 patients. Therefore, Ponti et al. [25] and Huyut [4] stated that the determination of effective routine laboratory biomarkers that can classify COVID-19 patients according to their fatal risk, supported by studies with large samples, is essential in order to guarantee rapid and effective treatment. Indeed, many studies have emphasized that the usefulness and effective breakpoints of many laboratory markers such as ferritin and D-dimer in predicting COVID-19 mortality have not been fully determined [11,17,26–28]. Therefore, Chalmers et al. [17] and Cheng et al. [29] stated that the predictive role of routine laboratory features in identifying risk factors affecting COVID-19 mortality needs further confirmation.

However, it is known that even the most knowledgeable and experienced physicians can interpret little of the information contained in routine blood laboratory results, and it is extremely difficult to determine the severity of COVID-19 patients based on laboratory findings alone [30]. In contrast, machine learning (ML) models have been successfully used to recognize subtle patterns in data to distinguish latent association patterns between routine blood parameters and disease [4,13,23,31,32] Indeed, several studies have shown that ML models can predict COVID-19 patient groups with high accuracy using patient demographics, physiological characteristics, and RBV data [33–36].

In our previous studies we determined routine blood values that predict the diagnosis and prognosis of COVID-19 with various supervised ML models and LogNNNet [4,5,13,23,32]. Huyut and Velichko [23] used only three RBV features with the LogNNNet model to predict the diagnosis and prognosis of COVID-19 disease. They achieved an accuracy of 99.17% in the diagnosis of the disease and an accuracy of 82.7% in determining the prognosis of the disease. Velichko et al. [32] achieved 100% accuracy in the diagnosis of COVID-19 using 11 RBV features with histogram-based gradient boosting model in their study. Huyut [4] classified severe and mild COVID-patients from a large patient population using 28 RBV features, and the models with the highest accuracy in classification were local weighted learning (97.86%) and k-nearest neighbor (94.05%).

Huyut and İlkbahar [5] used various biomarkers with the CHAID decision tree to detect the diagnosis and prognosis of COVID-19. The model produced 81.6% accuracy in recognizing the disease and 93.5% accuracy in determining the prognosis of the disease. Formica et al. [37] developed an ML model for early diagnosis of disease using 8 RBV features and reported 82% specificity with 83% sensitivity; however, the analysis is based on a small sample (171 patients). Banerjee et al. [38] classified a patient cohort of 598 cases, 39 of whom were COVID-19 positive, by various ML methods using 12 RBV features and reported good specificity (91%) but very low sensitivity (43%). Avila et al. [39] developed a Bayesian model using the dataset of using 12 RBV features and reported a sensitivity and specificity of 76.7% in the diagnosis of the disease. Joshi et al. [40] developed a trained logistic regression model using only hemogram data on a dataset of 380 cases and reported a 93%-sensitivity but low 43%-specificity in the diagnosis of COVID-19 disease. Zhu et al. [41] used 78 features consisting of demographic, clinical and RBV values with a deep neural network model to predict the mortality of COVID-19. They found the success of the method in diagnosis to be 95.4%-AUC. Soltan et al. [42] ran models of multivariate logistic regression, random forests and extreme gradient supported trees on more than 50 RBV data to identify COVID-19. The most successful model in the diagnosis of the disease was the XGBoost method with 85% sensitivity and 90% accuracy. Soares [43] developed an ML model using 15 RBV parameters to diagnose COVID-19 on a sample of 599 people, 81 of whom had positive COVID-19. Combining the SVM, ensemble and SMOTE Boost models, this model had 86% specificity and 70% success in diagnosing the disease.

In this study, 34 routine blood values were determined with a statistical approach in order to find the most successful ML classifier model in detecting patients with COVID-19 who lived and died. Then, 16 ML models were run with these features and the most successful model (histogram-based gradient boosting / HGB) was determined. The predictors of mortality of COVID-19 disease were revealed with the HGB model. The performance of individual and binary combinations of these predictors in detecting patient groups was obtained with the HGB model. In addition, correlations that between patient groups and binary combinations of features were interpreted in detail. In addition, cut-off values for these characteristics (mortality risk levels) were calculated by one and two-threshold approaches in the classification of patient groups according to direct characteristics. We think that the findings of this study will be an important motivation tool for clinicians in estimating the mortality of COVID-19 and detecting severe patients.

The paper has the following structure. Chapter 2 describes the data collection procedure, metrics, characteristics of the participants, the feature selection procedure, the one- and two-threshold approaches for classification based on the values of direct features, and a new  $F1^2$  criterion for the classification metric. Chapter 3 describes the correlations of features with patient groups, statistical differences of features between groups, classification results according to ML models, classification results of individual and pairwise combinations of features operated with the HGB model, classification results according to one- and two-threshold values of the features. Chapter 4 discusses the results and compares them with known developments. Chapter 5 presents the limitations of the study.

Finally, in Chapter 6, a general description of the study and its scientific significance are given.

## 2. Materials and Methods

In this retrospective-cohort study, data suitable for our criteria were collected from the Erzincan Binali Yildirim University Mengücek Gazi Training and Research Hospital information system between August and November 2021 and included in the study. The laboratory data of the patients were the routine blood values measured at the time of admission to the hospital. The information of the patients was followed up until exit and exit information was recorded. In our hospital, a diagnosis of SARS-CoV-2 was made by real-time reverse transcriptase polymerase chain reaction (RT-PCR) only on nasopharyngeal or oropharyngeal swabs.

### 2.1. Measurements

The hemogram data of the patients were studied in the biochemistry laboratory with the Sysmex XT4000i device and the biochemical tests with the Beckman Coulter AU2700 device. All patient data were double checked and analyzed by the research team. The hemogram data of the patients were studied in the biochemistry laboratory with the Sysmex XN-1000 device and the biochemical tests with the Beckman Coulter AU2700 device. Prothrombin time (PT), activated partial prothrombin time (aPTT), and fibrinogen were determined with a digital coagulation device from Ceveron-Alpha (Diapharma Group Inc., West Chester, Canada). The erythrocyte sedimentation rate (ESR) was measured using the TEST 1 BCL instrument (Alifax, Italy) based on the principle of photometric capillary flow kinetic analysis. Ferritin was evaluated with a chemiluminescence immunoassay (Centaur XP, Germany). C-reactive protein (CRP) was measured by nephelometric method in the BNTM II System (Siemens, Germany). Procalcitonin (PCT), D-dimer and Troponin were analyzed from whole blood on the AQT90 flex RadiometerVR (Denmark). All patient data were double checked and analyzed by the research team.

### 2.2. Characteristic of Participants and Define Datasets

In this study, only RBV data (features) of 2597 patients who were diagnosed with COVID-19 and treated at the hospital during the specified dates were used. During the treatment period, 233 (9.0%) of these patients died, while 2364 (91.0%) survived. Of the patients who lost their lives, 143 (61.3%) were male, while 90 (38.7%) were female. The mean age of the surviving patients was 55.00, while the mean age of the deceased patients was 76.00.

The routine laboratory information of these patients was examined. RBVs (features) that were measured from at least 80% of the patients were used. Missing data in this study were completed with the mean of the relevant parameter distribution and outliers were normalized. 38 routine blood values calibrated from approximately 70 parameters were used in this study. The data used in this study will be used as "SARS-CoV-2-RBV3". The SARS-CoV-2-RBV3 dataset includes immunological, hematological and biochemical parameters (Table 1).

These patients were of Turkish and Kurdish race. Only data of individuals over the age of 18 were recorded. Since it is a retrospective study, comorbidity data of the patients could not be obtained. In the SARS-CoV-2-RBV3 dataset, surviving patients were coded as 0 and patients who died were coded as 1 (survived COVID-19=0, non-survived COVID-19=1).

The features in this dataset are calibrated and include almost all of the RBV values that are the subject of studies on COVID-19 mortality. Therefore, we think that the bias of our study using this data set was minimized in comparison with the literature. In addition, the use of our data set, which we can share upon request from researchers, is important in terms of demonstrating the reproducibility and auditability of the results.

**Table 1.** Feature numbering for SARS-CoV-2-RBV3 dataset.

No	Feature	No	Feature	No	Feature	No	Feature
1	ALT	11	LDH	21	MCV	31	Ferritin
2	AST	12	eGFR	22	MONO	32	Fibrinogen
3	Albumin	13	UA	23	MPV	33	INR
4	ALP	14	BASO	24	NEU	34	PT
5	Amylase	15	EOS	25	PLT	35	PCT
6	CK-MB	16	HCT	26	RBC	36	ESR
7	D-Bil	17	HGB	27	RDW	37	Troponin
8	Glucose	18	LYM	28	WBC	38	aPTT
9	Creatinine	19	MCH	29	CRP		
10	CK	20	MCHC	30	D-dimer		

ALT: alanine aminotransaminase; AST: aspartate aminotransferase; ALP: Alkaline phosphatase: alkaline phosphatase; CK.MB: creatine kinase myocardial band; D-Bil: Direct Bilirubin; CK: Creatinine Kinase; LDH: lactate dehydrogenase; eGFR: estimating glomerular filtration rate; UA: uric acid; BASO: basophil count; EOS: eosinophil count; HCT: hematocrit; HGB: hemoglobin; LYM: lymphocyte count; MCH: mean corpuscular hemoglobin; MCHC: mean corpuscular hemoglobin concentration; MCV: mean corpuscular volume; MONO: monocyte count; MPV: mean platelet volume; NEU: neutrophil count; PLT: platelet count; RBC: red blood cells; RDW: red cell distribution width; WBC: white blood cell count; CRP: C-reactive protein; INR: international normalized ratio; PT: prothrombin time; PCT: Procalcitonin; ESR: erythrocyte sedimentation rate; aPTT: activated partial prothrombin time.

### 2.3. Feature selection for ML models with statistical approach.

In order to evaluate the difference of 38 RBV values between patients who survived and died from COVID-19, the assumptions of parametric tests were checked first. Since these assumptions were not met, the significance of the difference of 38 features between the patient groups was analyzed with the Mann-Whitney U test and p-values were calculated. 34 features were statistically different between patient groups and these features were used by ML models for classification. It has been understood that the features selected with this approach may be the determining factors between patients who died clinically and patients who survived. In addition, the use of clinically different features between patient groups by ML models increased the reliability of our results and reduced biased results.

### 2.4. Threshold approach

The simplest approach for classifying by one feature in the presence of only two classes is based on determining the threshold values separating the classes  $V_{th}$ .

*One threshold approach:*

For one threshold approach for the SARS-CoV-2-RBV3 dataset, we introduce the type of threshold value Type 1 or Type 2 in accordance with the rule:

$$\left\{ \begin{array}{l} \text{Type 1: if feature value} \geq V_{th} \text{ then "survived" else "non - survived COVID - 19"} \\ \text{Type 2: if feature value} \geq V_{th} \text{ then "non - survived" else "survived COVID - 19"} \end{array} \right.$$

The threshold type indicates which side of the threshold the non-survived and survived classes are on.

*Two threshold approach:*

For two threshold approach for the SARS-CoV-2-RBV3 dataset, we introduce the type of threshold value Type 1 or Type 2 in accordance with the rule:

- Type 1: if feature (value  $\geq V_{th_1}$ ) and (value  $\leq V_{th_2}$ ) then "survived" else "non - survived COVID -19"
- Type 2: if feature (value  $\geq V_{th_1}$ ) and (value  $\leq V_{th_2}$ ) then "non - survived" else "survived COVID -19"

The main metrics were calculated after balancing datasets. K-fold validation is not used when calculating  $A_{th}$  and  $F1^2$ . The threshold values  $V_{th}$ ,  $V_{th_1}$ ,  $V_{th_2}$  was determined by stepwise enumeration and finding the maximum value of  $A_{th}$ .

### 2.5. $F1^2$ metric

To select the most significant features, we introduced an additional metric  $F1^2$  equal to the product of the F1 metrics of two classes.

$$F1^2 = F1(\text{non - survived COVID -19}) \cdot F1(\text{survived COVID -19}) \quad (1)$$

## 3. Results

### 3.1. Correlation analysis of Dataset SARS-CoV-2-RBV3

Figure 1 shows the results of the correlation analysis of the diagnosis - feature using the three types of Pearson, Spearman and Kendall correlations over the entire volume of the SARS-CoV-2-RBV3 database. It can be seen that the Spearman and Kendall correlations have very similar values. The Pearson correlation gives in general a smaller number of features that correlate with the diagnosis, so we will use the Spearman correlation as the main one.

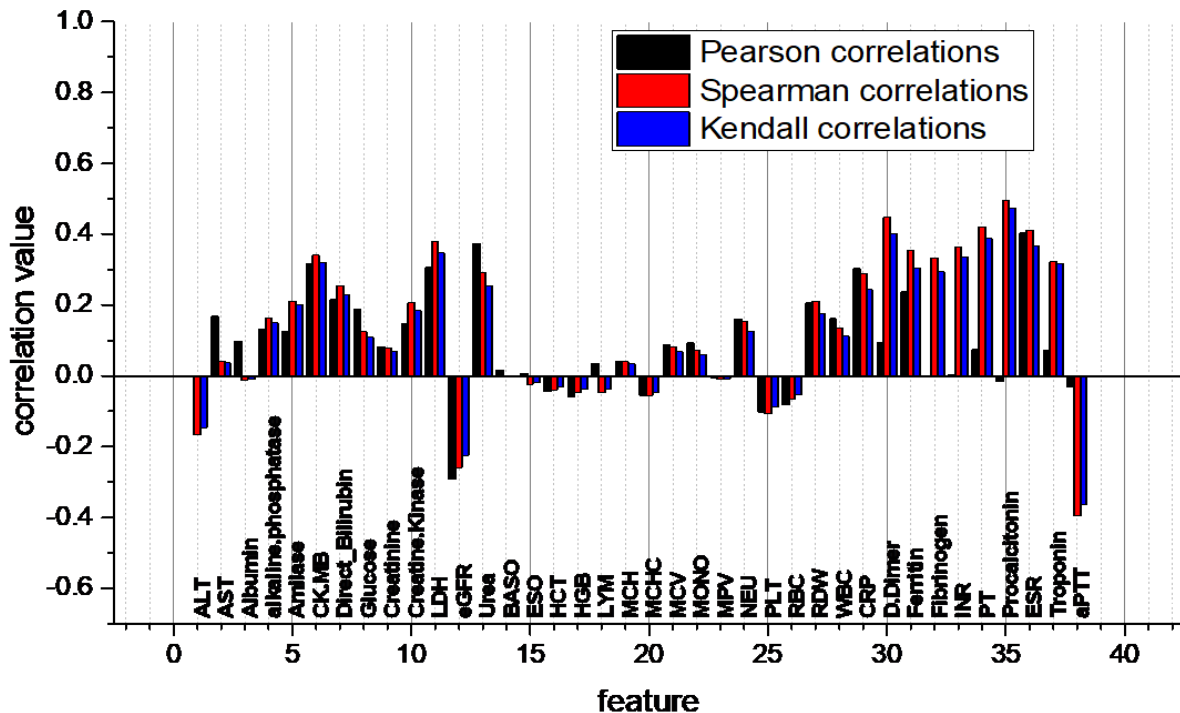
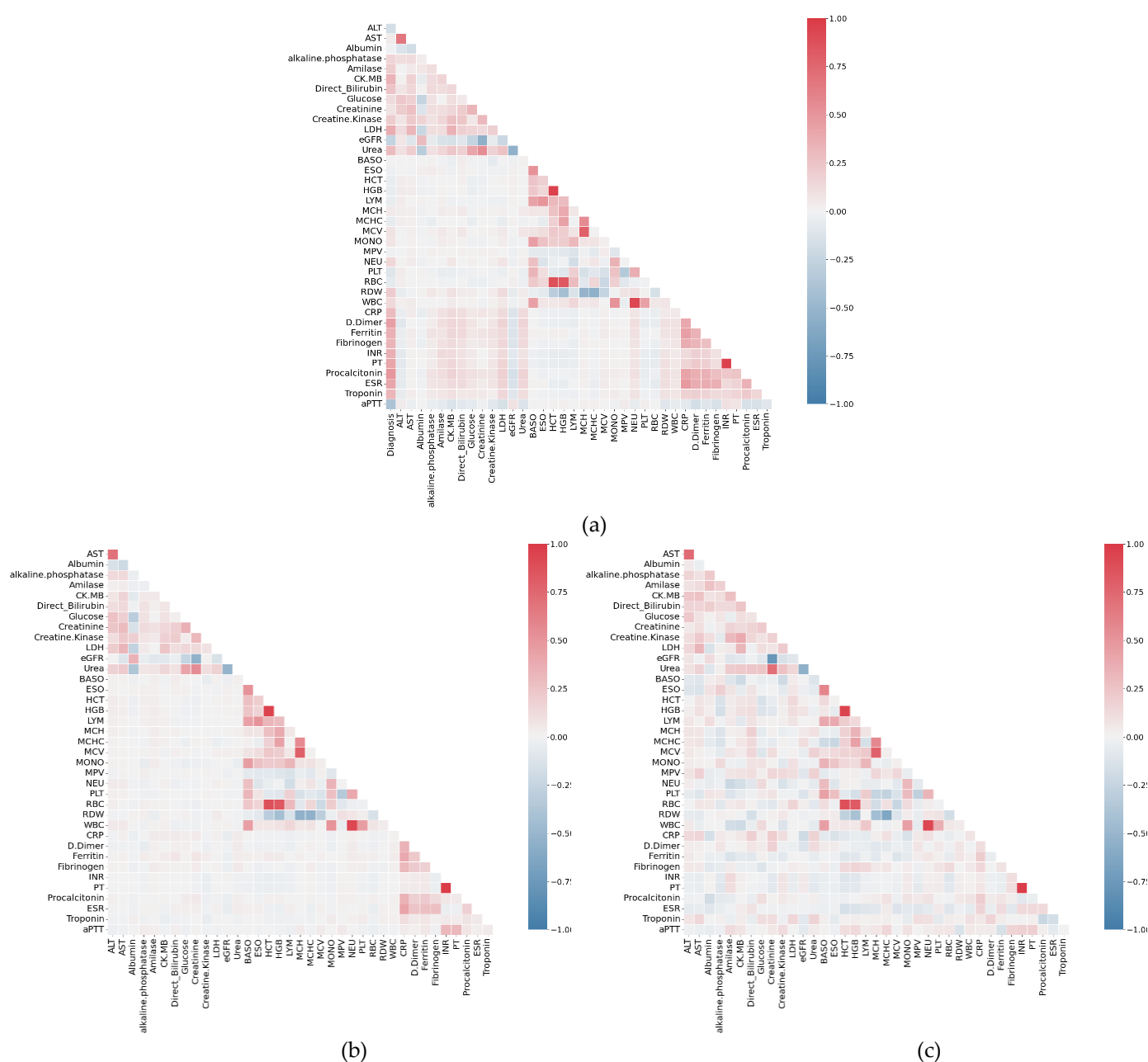


Figure 1. Pearson, Spearman and Kendall correlations of the SARS-CoV-2-RBV3 dataset for COVID-19 mortality - feature pairs.



**Figure 2.** Spearman correlation analysis results for the entire database (a), survived COVID-19 class (b) and non-survived COVID-19 class (c) from the SARS-CoV-2-RBV3 dataset.

Full Spearman heatmaps across the entire database and by class (survived COVID-19 and non-survived COVID-19) are shown in Figure 2.

Figures 2bc show that the non-survived COVID-19 class is characterized by an increased correlation between features compared to the survived COVID-19 class, which indicates poor self-regulation in the body.

The most significant changes in the correlation of features of the non-survived COVID-19 class compared with the survived COVID-19 class are presented in Table 2. Here, the qualitative change is denoted as ‘Down’ and ‘Up’. For some pairs of features, the correlation increased, for some it fell.

**Table 2.** Changes in the correlation of feature pairs of the non-survived COVID-19 class compared with the survived COVID-19 class.

No	No	Spearman survived COVID-19	Spearman non-survived COVID-19	Change in the correlation of features, in present of non-survived COVID-19	Feature	Feature
8	3	-0.31194	0.01274	Down	Glucose	Albumin
13	3	-0.3753	-0.10287	Down	Urea	Albumin
36	29	0.42911	0.16647	Down	ESR	CRP
10	5	0.05417	0.30605	Up	Creatine.Ki-nase	Amilase
12	9	-0.53482	-0.77476	Up	eGFR	Creatinine
5	3	-0.03084	0.26142	Up	Amilase	Albumin
12	3	0.3479	0.11987	Down	eGFR	Albumin
30	29	0.3365	0.1146	Down	D.Dimer	CRP
6	5	0.05413	0.26867	Up	CK.MB	Amilase
32	30	0.21431	-1.48572E-4	Down	Fibrinogen	D.Dimer
10	6	0.18243	0.39221	Up	Creatine.Ki-nase	CK.MB
36	30	0.25085	-0.04489	Down	ESR	D.Dimer
24	5	0.00641	-0.21234	Up	NEU	Amilase
14	6	-0.00966	-0.20355	Up	BASO	CK-MB
4	3	-0.03222	0.22455	Up	ALT	Albumin
26	18	0.30758	0.1153	Down	RBC	LYM
9	1	0.24486	0.05265	Down	Creatinine	ALT
16	15	0.20104	0.01024	Down	HCT	ESO
9	2	0.30293	0.1127	Down	Creatinine	AST
17	14	0.24856	0.05841	Down	HGB	BASO
25	15	0.0849	0.27473	Up	PLT	ESO
25	20	-0.08083	-0.27021	Up	PLT	MCHC
7	3	-0.0119	0.19865	Up	D-Bil	Albumin
20	15	-0.04499	-0.23071	Up	MCHC	ESO
31	29	0.3931	0.2085	Down	Ferritin	CRP
28	6	0.0179	-0.20122	Up	WBC	CK-MB
27	21	-0.30218	-0.11908	Down	RDW	MCV
7	6	0.0635	0.24642	Up	D-Bil	CK.MB
36	32	0.27287	-0.09309	Down	ESR	Fibrinogen
20	14	0.02204	-0.1999	Up	MCHC	BASO
13	8	0.42328	0.24648	Down	Urea	Glucose
15	4	0.01565	0.19167	Up	ESO	ALT
31	30	0.22095	-0.04543	Down	Ferritin	D-dimer
6	1	0.06557	0.23993	Up	CK-MB	ALT
32	29	0.31919	0.14655	Down	Fibrinogen	CRP
23	2	0.00857	0.18043	Up	MPV	AST
3	2	-0.20943	-0.03802	Down	Albumin	AST
35	3	-0.01609	-0.18485	Up	PCT	Albumin
30	9	-0.00743	0.17441	Up	D-dimer	Creatinine
23	13	0.00586	0.1727	Up	MPV	Urea



### 3.2. Comparison of RBV features of surviving and non-surviving COVID-19 patients and Comparison of ML classifiers

The statistical comparison results of 38 characteristics of surviving and non-surviving COVID-19 patients are presented in Table 3. Except for albumin, BASO, EOS and MPV, the other 34 features were statistically different between the patient groups. The 34 features selected here were used as inputs to identify patient groups with ML models, and the classification performance of the models was obtained (Table 4 and Figure 3). Considering the  $F1^2$  (see equation 1) criterion derived from the F1 metrics of the classes in the classification of patient groups, it was found that the most successful model was HGB ( $F1^2$  value: 1). After HGB, the most successful models were Adaboost, Extra Trees, KNN, RF, SVM-LK, (at least  $F1^2 > 0.99$  in these models). The most unsuccessful model was Quadratic Discriminant Analysis ( $F1^2$  value: 0.72).

**Table 3.** Descriptive statistics of RBV values of groups surviving and non-surviving from COVID-19

	Surviving Group			non-Surviving Group			p
	Median	Percentile 25	Percentile 75	Median	Percentile 25	Percentile 75	
ALT	35.31	24.00	35.31	23.00	15.00	35.20	<.000
AST	33.24	25.00	33.24	32.00	22.00	47.23	.033
Albumin	38.59	38.59	38.59	38.29	33.00	43.54	.539
ALP	84.10	84.10	84.10	103.23	72.00	103.23	<.000
Amilase	73.70	73.70	73.70	101.00	58.00	107.62	<.000
CK-MB	18.79	18.79	18.79	32.75	19.40	32.75	<.000
D-Bil.	.13	.13	.13	.25	.12	.27	<.000
Glucose	136.03	108.00	136.03	145.00	113.00	188.00	<.000
Creatinine	1.14	.90	1.14	1.11	.86	1.64	<.000
CK	104.26	83.00	104.26	220.00	79.00	350.53	<.000
LDH	252.94	252.94	252.94	309.76	309.76	309.76	<.000
eGFR	82.74	82.74	85.10	62.16	44.47	82.50	<.000
Urea	38.80	32.00	38.80	56.74	39.13	75.95	<.000
BASO	.02	.01	.04	.021	.014	.044	.869
EOS	.04	.01	.12	.03	.00	.12	.232
HCT	39.55	36.00	43.20	38.80	34.90	42.30	.041
HGB	13.30	12.00	14.65	13.10	11.50	14.50	.016
LYM	1.46	.99	2.03	1.32	.85	1.88	.015
MCH	28.60	27.30	29.60	28.80	27.20	30.10	.041
MCHC	33.80	32.90	34.70	33.50	32.40	34.60	.004
MCV	83.90	80.80	87.00	85.20	81.80	88.90	<.000
MONO	.51	.38	.67	.56	.44	.72	<.000
MPV	10.30	9.70	10.90	10.30	9.60	11.00	.604
NEU	4.05	2.85	5.85	5.25	3.98	7.65	<.000
PLT	229,00	184,00	287,00	200,00	166,00	250,00	<.000
RBC	4.74	4.36	5.14	4.64	4.16	4.98	.001
RDW	13.10	12.50	13.90	14.00	13.20	15.40	<.000
WBC	6.50	5.00	8.30	7.80	6.20	10.10	<.000

CRP	6,76	3,02	23,50	72,00	17,10	72,00	<.000
D-dimer	441,00	441,00	441,00	1277,00	1277,00	1277,00	<.000
Ferritin	125,95	90,90	175,80	395,00	395,00	395,00	<.000
Fibrinogen	321,10	321,10	321,10	350,00	350,00	350,00	<.000
INR	1,10	1,10	1,10	1,20	1,20	1,20	<.000
PT	13,10	13,10	13,10	14,20	14,20	14,20	<.000
PCT	,12	,12	,12	2,75	2,53	2,75	<.000
ESR	17,00	17,00	17,00	49,00	49,00	49,00	<.000
Troponin	16,12	10,00	19,00	53,27	15,00	75,00	<.000
aPTT	32,75	32,75	32,75	32,00	32,00	32,00	<.000

p<0.05 was considered significant.

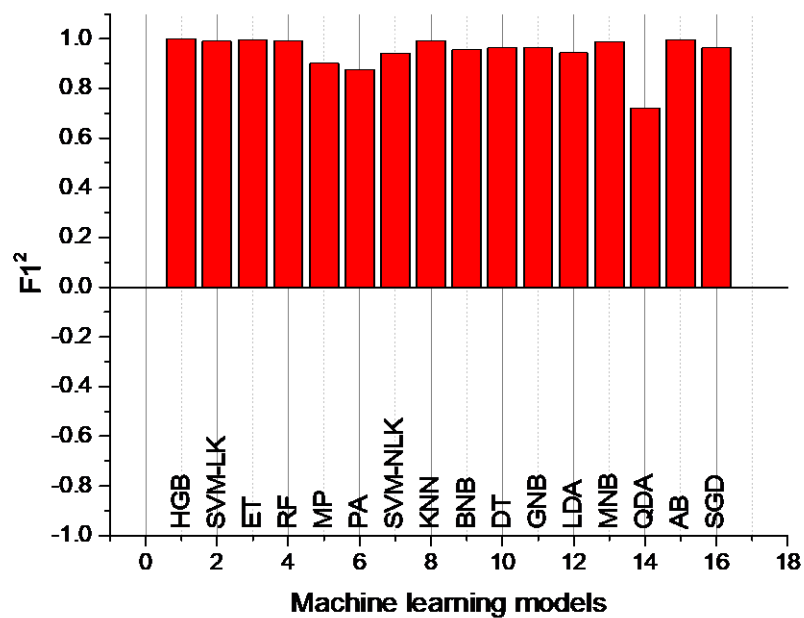


**Figure 3.** Performance of ML models in classifying surviving and non-surviving COVID-19 patients using the 34 features.

**Table 4.** Classification performance of ML models run with 34 features to detect patient groups.

No	ML models	F1²
1	Histogram based Gradient Boosting (HGB)	1.0000
2	Adaboost (AB)	0.9952
3	Extra Trees (ET)	0.9952
4	K nearest neighbors (KNN)	0.9929
5	Random Forest (RF)	0.9928
6	Support Vector Machine with Linear Kernel (SVM-LK)	0.9904
7	Multinomial Naive Bayes (MNB)	0.9881
8	Gaussian Naive Bayes (GNB)	0.9646
9	Stochastic Gradient Descent (SGD)	0.9642
10	Decision Tree (DT)	0.9642

11	Bernoulli Naive Bayes (BNB)	0.9563
12	Linear discriminant analysis (LDA)	0.9431
13	Support Vector Machine with non-linear Kernel (SVM-NLK)	0.9428
14	Multilayer Perceptron (MP)	0.9011
15	Passive-Aggressive (PA)	0.8772
16	Quadratic Discriminant Analysis (QDA)	0.7212

### 3.3. Investigation of the effectiveness of the models operating on the one- feature HGB model

It is known that the use of the F1 score may be more useful than the accuracy value in cases where the data distributions are not equal. Figure 4 shows a comparison of F1 metrics for the survived COVID-19 class calculated for the original and Smote balanced datasets. It can be seen that, for survived COVID-19, there is a high F1 value for all features for both databases.

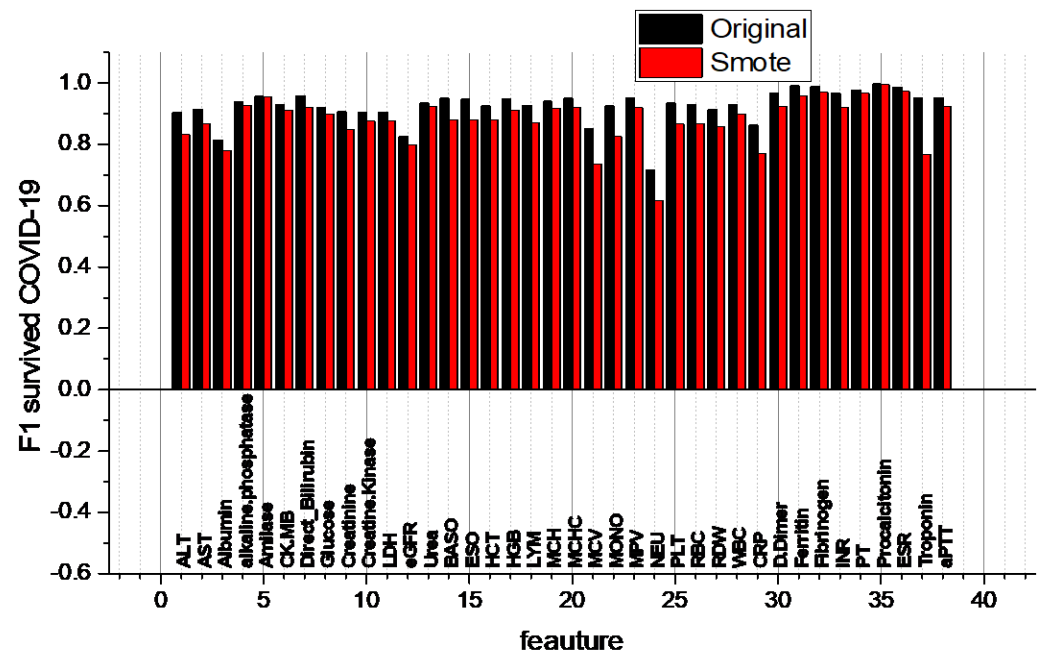


**Figure 4.** F1 metrics for survived COVID-19 class, calculated for original and Smote balanced datasets.

Figure 5 shows a comparison of F1 metrics for the non-survived COVID-19 class calculated for the original and Smote balanced datasets. It can be seen that, for non-survived COVID-19, a high F1 value is observed for most of the features for Smote balanced datasets, while for the original dataset, only a part of the features have a high F1. Thus, to select main features, it is logical to use the results of calculating the metrics for the original dataset. Synthetic data, although well approximated by the model, nevertheless does not allow us to judge the performance of the model with real data. Table A1 in Appendix presents the classification result of SARS-CoV-2-RBV3 datasets for the HGB model using a single input feature for original datasets, indicating the main classification metrics (Precision, Recall, F1).

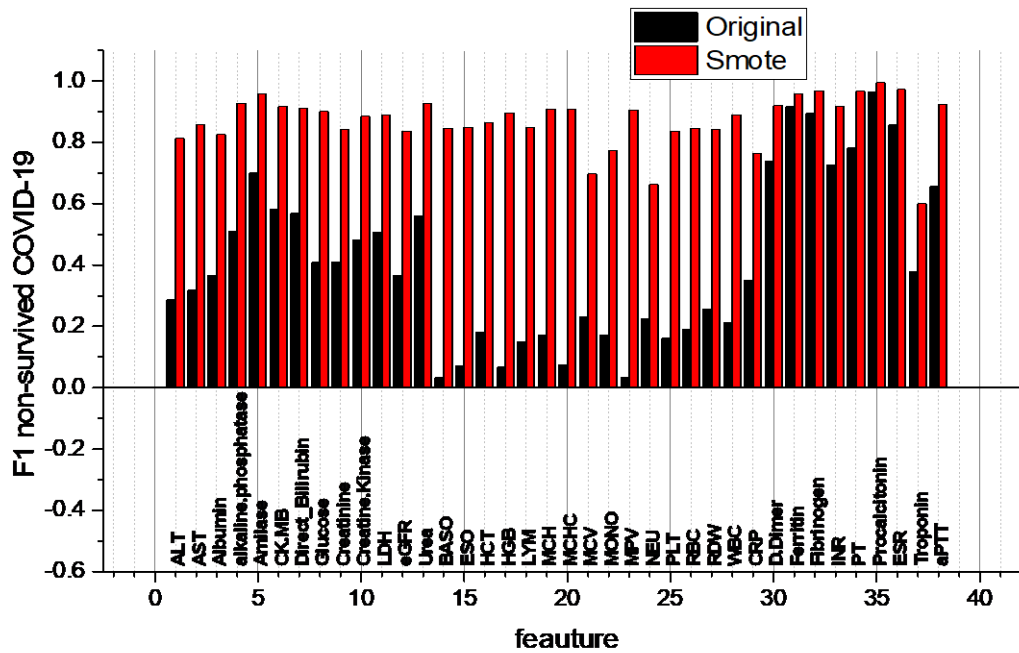


**Figure 5.** F1 metric for non-survived COVID-19 class, calculated for original and Smote balanced datasets.

### 3.4. $F1^2$ metric in the detection of patient groups with the HGB model, one-threshold and two-threshold approaches

Figure 6 shows the dependence of  $F1^2$  on the feature. Let us agree to consider as the most significant features those features in which  $F1^2 \geq 0.5$ , this threshold is visualized in the figure by the blue line.

As a result, we get a list of the 12 most significant single features for HGB classification, shown in Table 5., in which  $F1^2 \geq 0.5$ . No high  $F1^2$  value was found in the classification of patient groups with the single-threshold value approach. However, high  $F1^2$  values were found in the classification of patient groups with the HGB model operated with a single feature and the two-threshold value approach. Accordingly, PCT and ferritin properties were found to be the most effective in classification according to the HGB model operated with one feature and the two-threshold approach.

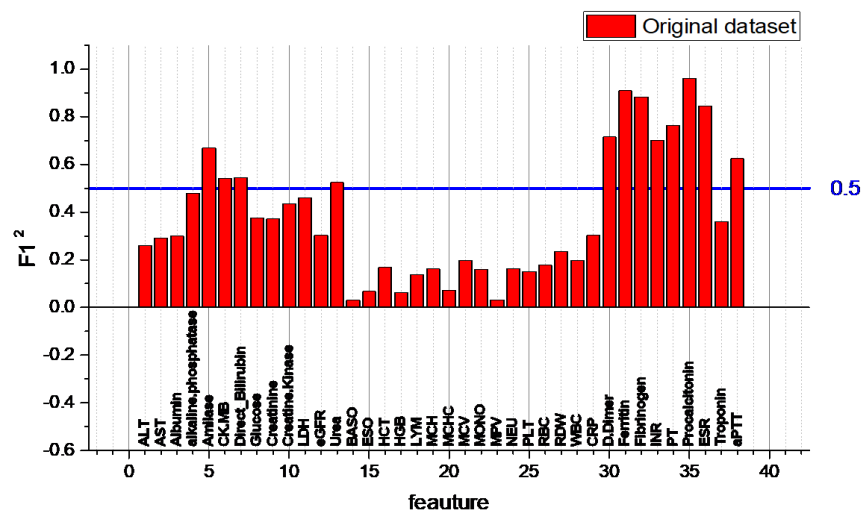


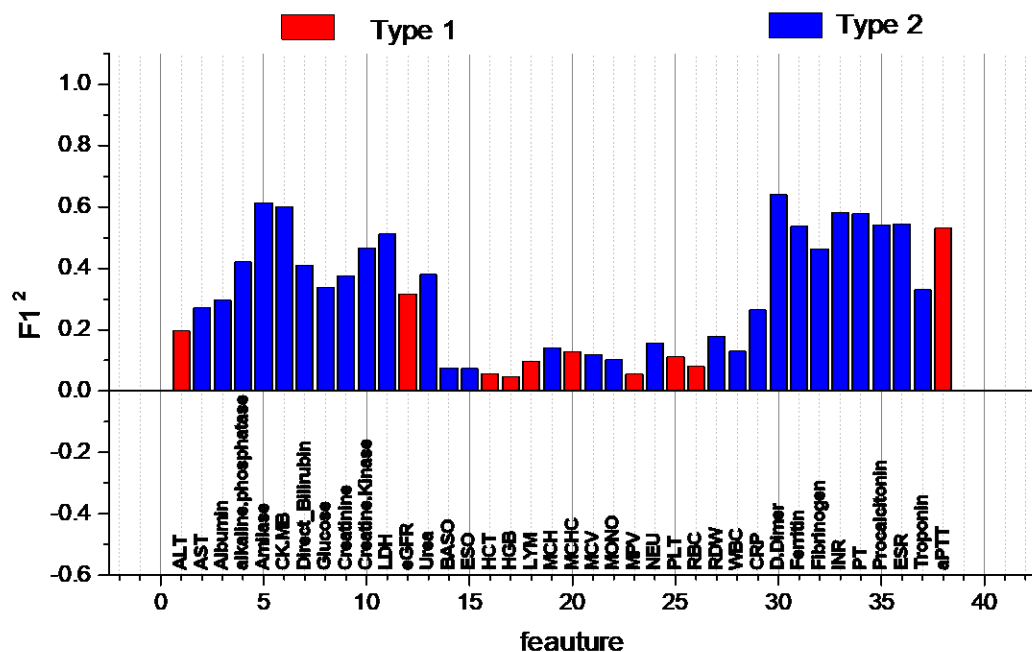
**Figure 6.**  $F1^2$  metric of the HGB model according to each feature for the detection of surviving and non-surviving COVID-19 patients.

**Table 5.** List of the 12 most significant single features for classification by the HGB algorithm, with  $F1^2$  metric.

Feature name	№	$F1^2$ HGB Model	$F1^2$ One threshold approach	$F1^2$ Two threshold approach
PCT	35	0.9621	0.54277	0.95118
Ferritin	31	0.90966	0.53731	0.90577
Fibrinogen	32	0.88417	0.4635	0.67443
ESR	36	0.845	0.54522	0.69842
PT	34	0.76401	0.579	0.58245
D-dimer	30	0.71535	0.6408	0.65008
INR	33	0.70204	0.58302	0.58743
Amilase	5	0.6699	0.61374	0.6599
aPTT	38	0.62451	0.53117	0.53603
D-Bil	7	0.54567	0.41042	0.4068
CK-MB	6	0.54277	0.6026	0.46247
Urea	13	0.52454	0.38088	0.38088

### Threshold Approach

For one threshold approach, we obtained the distribution of the  $F1^2$  metric shown in Figure 7. Model types are marked with color (Type 1, Type 2). The complete collection of metrics (Type,  $V_{th}$ ,  $A_{th}$ , Precision, Recall, F1,  $F1^2$ ) is presented in Table A2 of the Appendix.

**Figure 7.** The  $F1^2$  metric for the classification of surviving and non-surviving COVID-19 patients according to a single feature for the one-threshold approach. With dependency type visualization (Type 1, Type 2).

For two threshold approach, we obtained the distribution of the  $F1^2$  metric shown in Figure 8. Model types are marked with color (Type 1, Type 2). The complete collection of metrics (Type,  $V_{th1}$ ,  $V_{th2}$ ,  $A_{th}$ , Precision, Recall, F1,  $F1^2$ ) is presented in Table A3 of the Appendix.

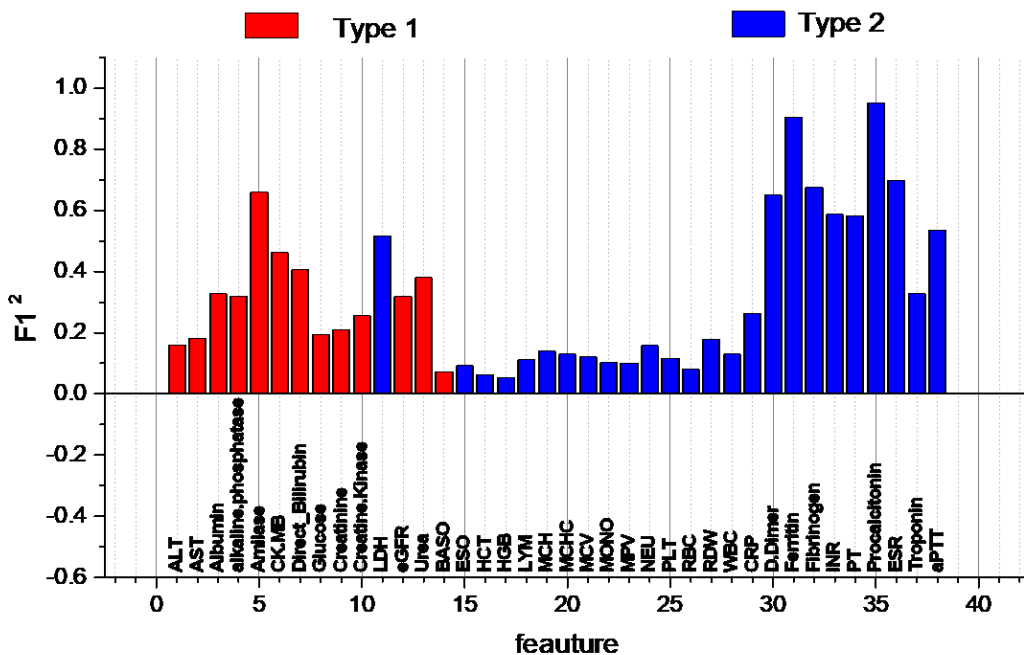


Figure 8. The F1<sup>2</sup> metric for the classification of surviving and non-surviving COVID-19 patients according to a single feature for the two-threshold approach. With dependency type visualization (Type 1, Type 2).

Procalcitonin, ferritin, and fibrinogen sample for the histogram distributions and classification results of the characteristics of surviving and non-surviving COVID-19 patients according to the one-threshold approach are shown in Fig 9.

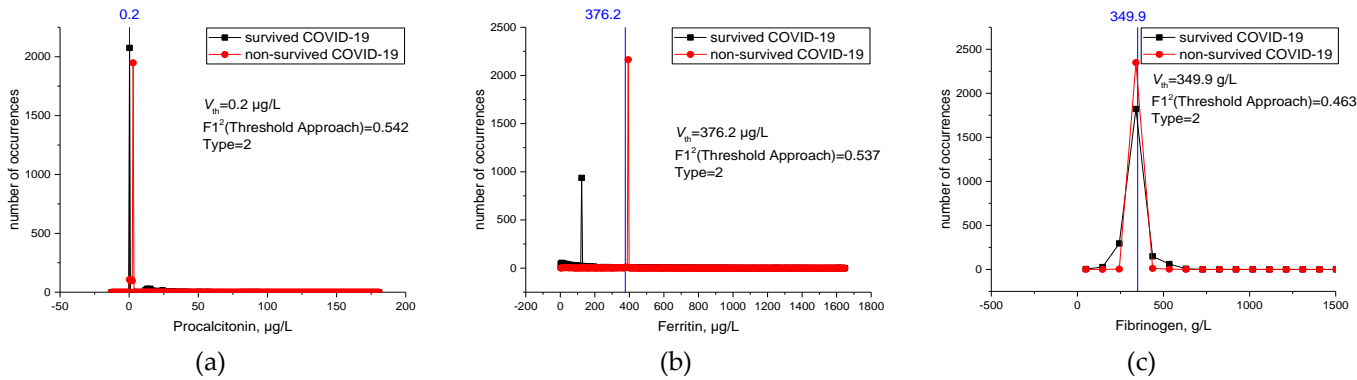
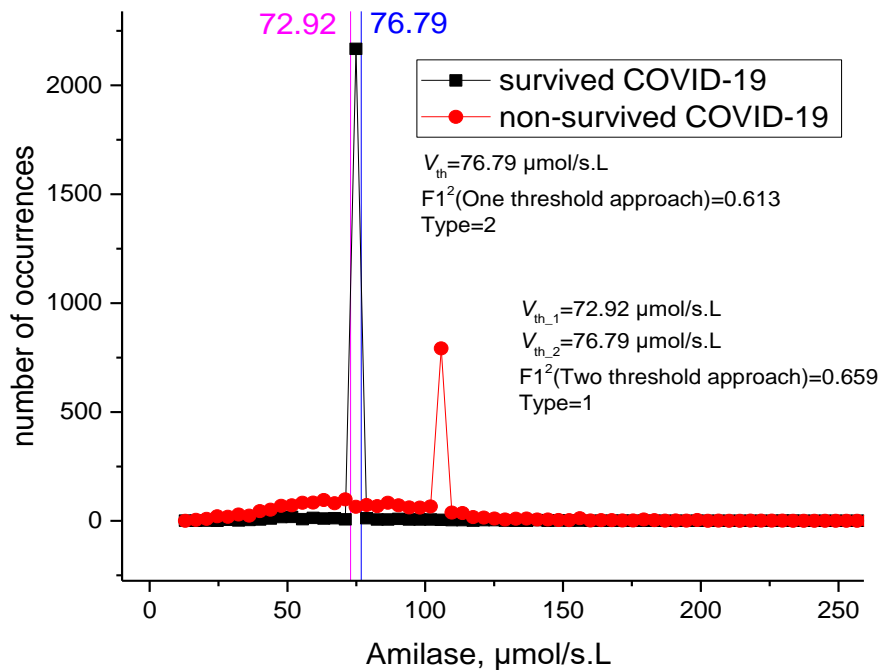


Figure 9. Histogram distributions and F1<sup>2</sup> result of procalcitonin (a), ferritin (b) and fibrinogen (c) properties according to single-cut-off value approach in estimating COVID-19 mortality. V<sub>th</sub> (blue line) is the threshold for detecting COVID-19 mortality.

Amilase sample for the histogram distribution and classification result of the characteristics of surviving and non-surviving COVID-19 patients according to the two-threshold approach are shown in Fig 10.



**Figure 10.** Histogram distributions and  $F1^2$  result of amylase feature according to two-threshold value approach in estimating COVID-19 mortality.  $V_{th_1}$  (pink line) and  $V_{th_2}$  (blue line) is the threshold for detecting COVID-19 mortality.

Comparison of Spearman correlation and HGB model and Threshold Approach

It was observed that the performance of the HGB model with a single feature ( $F1^2$ ) in the classification of patient groups who died and survived from COVID-19 was more successful than the classification made by considering one and two threshold values (Figure 11). In addition, the approach of identifying patient groups based on the relationship structure of the characteristics with the patient groups (Spearman) produced the lowest results (Figure 11).

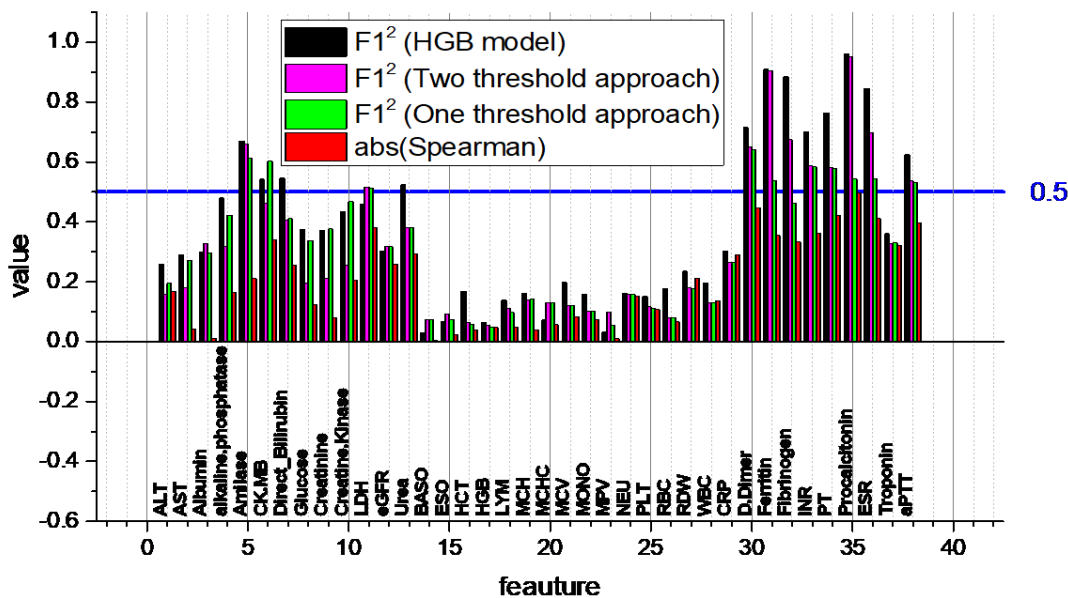


**Figure 11.**  $F1^2$  metric of SARS-CoV-2-RBV3 datasets for different models.

### 3.5. Investigation of the effectiveness of the HGB model working on two features for the detection of surviving and non-surviving COVID-19

For the detection of living and deceased COVID-19 patient groups, the Smote-trained HGB model was run with dual features and classification performances are presented in Table 4. In addition,  $F1^2$  values related to binary properties and classification performances operated with the HGB model are visualized in two-dimensional space (Figure 12).

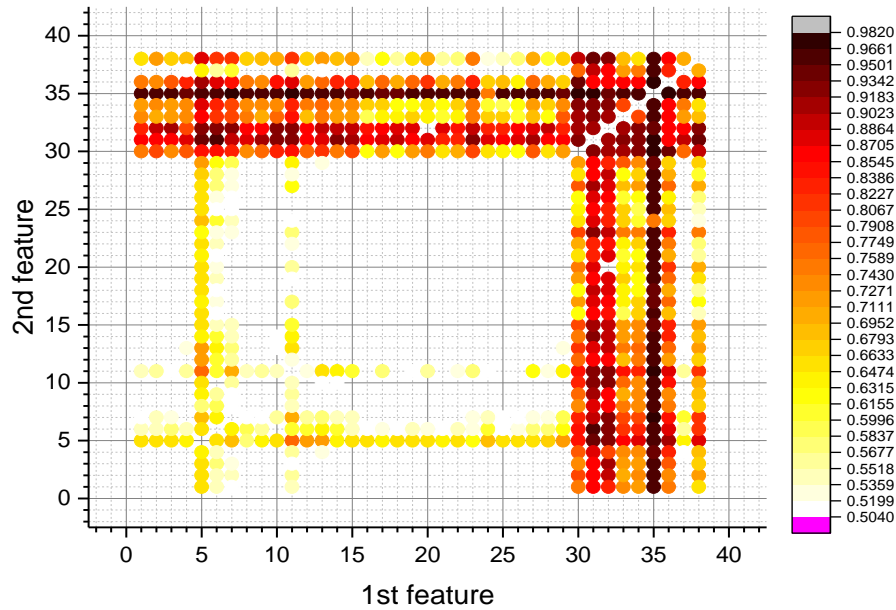


**Figure 12.** Feature pairs with the highest  $F1^2$  value that it was found with the HGB classifier for detection of surviving and non-surviving COVID-19 patients.

When Table 6 and Figure 12 are examined, the HGB model showed a classification performance of  $F1^2 = 0.98$  with only D-dimer and PCT couple in the detection of surviving and non-surviving patients. The classification performances of the feature pairs formed by PCT with ESR, DBil, Ferritin and LDH were approximately  $F1^2 = 0.98$ . Patients who both surviving and non-surviving with these trait pairs were identified with high precision and recall value. PCT appears to be the feature that most closely matches other features in predicting disease mortality. After PCT, it can be said that ferritin is the most matching property with other properties. In addition,  $\geq 0.94$   $F1^2$  values were found in the patient group classification of various trait pairs with the HGB model (Table 6)

Also, according to the two-threshold approach; It was found that the majority of patients who died had fibrinogen values between 349.98 g/L and 379.05 g/L ( $F1^2 = 0.68$ ), D-dimer values between 1009.99  $\mu\text{g/L}$  ile 10742.71  $\mu\text{g/L}$  ( $F1^2 = 0.65$ ), ESR values between 36.12 ile 56.62 ( $F1^2 = 0.70$ ), ferritin values between 376.2  $\mu\text{g/L}$  ile 396.0  $\mu\text{g/L}$  ( $F1^2 = 0.91$ ), and PCT values between 0.2  $\mu\text{g/L}$  and 5.2  $\mu\text{g/L}$  ( $F1^2 = 0.95$ ) [Fig 8 and Supplementary Table A3]. It can be said that the determined value ranges of these features are the most important lethal risk levels. It is noteworthy that procalcitonin and ferritin are the most important feature pairs in the detection of surviving and non-surviving COVID-19 patients, according to both the HGB classifier and the two-threshold approach.

**Table 6.** Feature pairs with the highest metrics that it was found with the HGB classifier for detection of surviving and non-surviving COVID-19 patients.

Feature pairs				Precision		Recall		F1		F1 <sup>2</sup>
				surv.	non-surv.	surv.	non-surv.	surv.	non-surv.	
D-dimer	PCT	30	35	0.9979	0.9867	0.9987	0.9786	0.9983	0.9825	0.98083
PCT	ESR	35	36	0.997	0.9911	0.9992	0.9704	0.9981	0.9805	0.97864
D-Bil	PCT	7	35	0.9987	0.9735	0.9975	0.9866	0.9981	0.9798	0.97794
Ferritin	PCT	31	35	0.997	0.9868	0.9987	0.9699	0.9979	0.9782	0.97615
LDH	PCT	11	35	0.9992	0.9648	0.9966	0.991	0.9979	0.9774	0.97535
PT	PCT	34	35	0.9953	0.9781	0.9979	0.9536	0.9966	0.9654	0.96212
PCT	aPTT	35	38	0.9975	0.9564	0.9958	0.975	0.9966	0.9643	0.96102
CK-MB	PCT	6	35	0.9983	0.9473	0.995	0.983	0.9966	0.9641	0.96082
INR	PCT	33	35	0.9941	0.9868	0.9987	0.9435	0.9964	0.9641	0.96063
MCH	PCT	19	35	0.9992	0.9386	0.9941	0.991	0.9966	0.9635	0.96022
ALT	PCT	1	35	0.9992	0.9386	0.9941	0.991	0.9966	0.9635	0.96022
MCV	PCT	21	35	0.9992	0.9386	0.9941	0.991	0.9966	0.9635	0.96022
eGFR	PCT	12	35	0.9992	0.9386	0.9941	0.991	0.9966	0.9635	0.96022
Creatinine	PCT	9	35	0.9992	0.9386	0.9941	0.991	0.9966	0.9635	0.96022
RBC	PCT	26	35	0.9992	0.9386	0.9941	0.991	0.9966	0.9635	0.96022
Glucose	PCT	8	35	0.9992	0.9386	0.9941	0.991	0.9966	0.9635	0.96022
Urea	PCT	13	35	0.9992	0.9386	0.9941	0.991	0.9966	0.9635	0.96022
WBC	PCT	28	35	0.9987	0.9386	0.9941	0.9863	0.9964	0.9614	0.95794
BASO	PCT	14	35	0.9987	0.9386	0.9941	0.9865	0.9964	0.9613	0.95784
PLT	PCT	25	35	0.9987	0.9386	0.9941	0.9865	0.9964	0.9613	0.95784
RDW	PCT	27	35	0.9987	0.9386	0.9941	0.9865	0.9964	0.9613	0.95784
AST	PCT	2	35	0.9987	0.9386	0.9941	0.9865	0.9964	0.9613	0.95784
PCT	Troponin	35	37	0.9983	0.9386	0.9941	0.9821	0.9962	0.9593	0.95565
CK	PCT	10	35	0.9979	0.9431	0.9945	0.978	0.9962	0.9593	0.95565
MPV	PCT	23	35	0.9983	0.9386	0.9941	0.9817	0.9962	0.9593	0.95565
MONO	PCT	22	35	0.9983	0.9386	0.9941	0.9819	0.9962	0.9593	0.95565
Albumin	PCT	3	35	0.9992	0.9297	0.9933	0.9912	0.9962	0.958	0.95436
MCHC	PCT	20	35	0.9987	0.9298	0.9933	0.9878	0.996	0.9566	0.95277
CK-MB	Ferritin	6	31	0.9924	0.987	0.9987	0.9271	0.9955	0.9558	0.9515
Amilase	PCT	5	35	0.9966	0.9474	0.995	0.9648	0.9958	0.9554	0.95139
HCT	PCT	16	35	0.9979	0.9343	0.9937	0.9792	0.9958	0.9549	0.95089
Ferritin	aPTT	31	38	0.9915	0.9825	0.9983	0.9258	0.9949	0.9511	0.94625
ESO	PCT	15	35	0.997	0.9343	0.9937	0.9688	0.9954	0.9506	0.94623
HGB	PCT	17	35	0.9979	0.9253	0.9929	0.9768	0.9954	0.9495	0.94513
LYM	PCT	18	35	0.9962	0.9386	0.9941	0.9604	0.9951	0.9488	0.94415
D-dimer	ESR	30	36	0.9911	0.9825	0.9983	0.9161	0.9947	0.9477	0.94268
CRP	PCT	29	35	0.9958	0.9386	0.9941	0.9579	0.9949	0.9468	0.94197

### 3.6. Concept of 1D and 2D masks

In order to understand the working principle of the HGB model in the classification of surviving and non-surviving COVID-19 patients, the cut-off values of one and two features and their sampling distributions were drawn and the results were visualized with the masking technique.

1D Mask of HGB model

Figure 12a shows the distribution of procalcitonin by patient groups on the original dataset and shows how the patient groups were classified according to the threshold values of this feature. The procalcitonin value is used as an example to understand the procedure for identifying patient groups according to a single feature of the HGB model. The classification results of the HGB model, which uses the cut-off values of procalcitonin to determine the patient groups, are visualized in the 1D mask technique in Figure 12b.

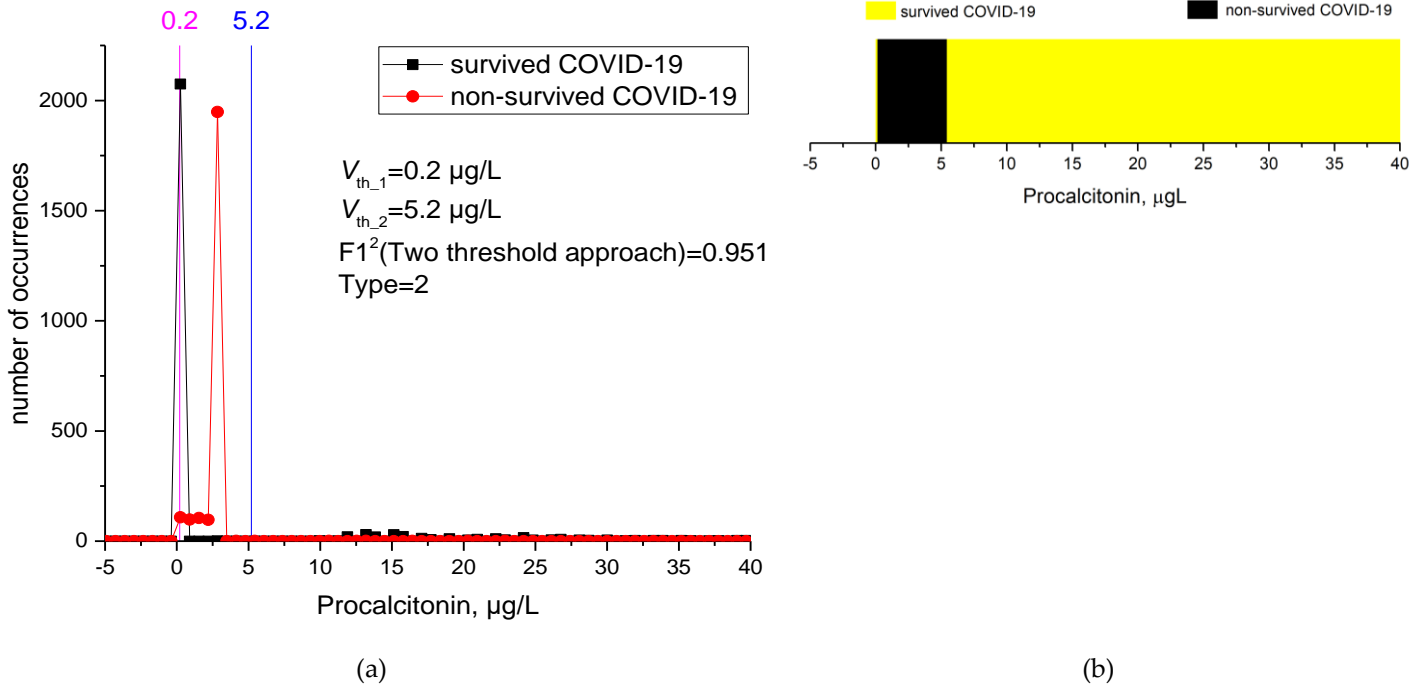


**Figure 12.** a) Distribution of the procalcitonin feature in the original data of patients who survived and died from COVID-19, and the two threshold value for this feature in classification. b) 1D masking technique for classifying patient groups of the HGB model operated with the procalcitonin feature.

#### 2D Mask of HGB model

Figure 13 a,c shows the distribution of D-dimer-ferritin and MCH-creatinine kinase properties in two-dimensional space according to patient groups on the original dataset. These feature pairs have been chosen as examples to understand the working principle of the HGB model with dual features. The results of classification of living and deceased COVID-19 patients with the HGB model using these features were visualized with the 2D masking technique (Figure 13 b,d). D-dimer-ferritin properties were the feature pairs with the highest  $F1^2$  score in the identification of patient groups with HGB, while MCH-Creatinine kinase was the feature pairs with the lowest  $F1^2$  score. Here we have shown the working principle of these two contrasting features with HGB.

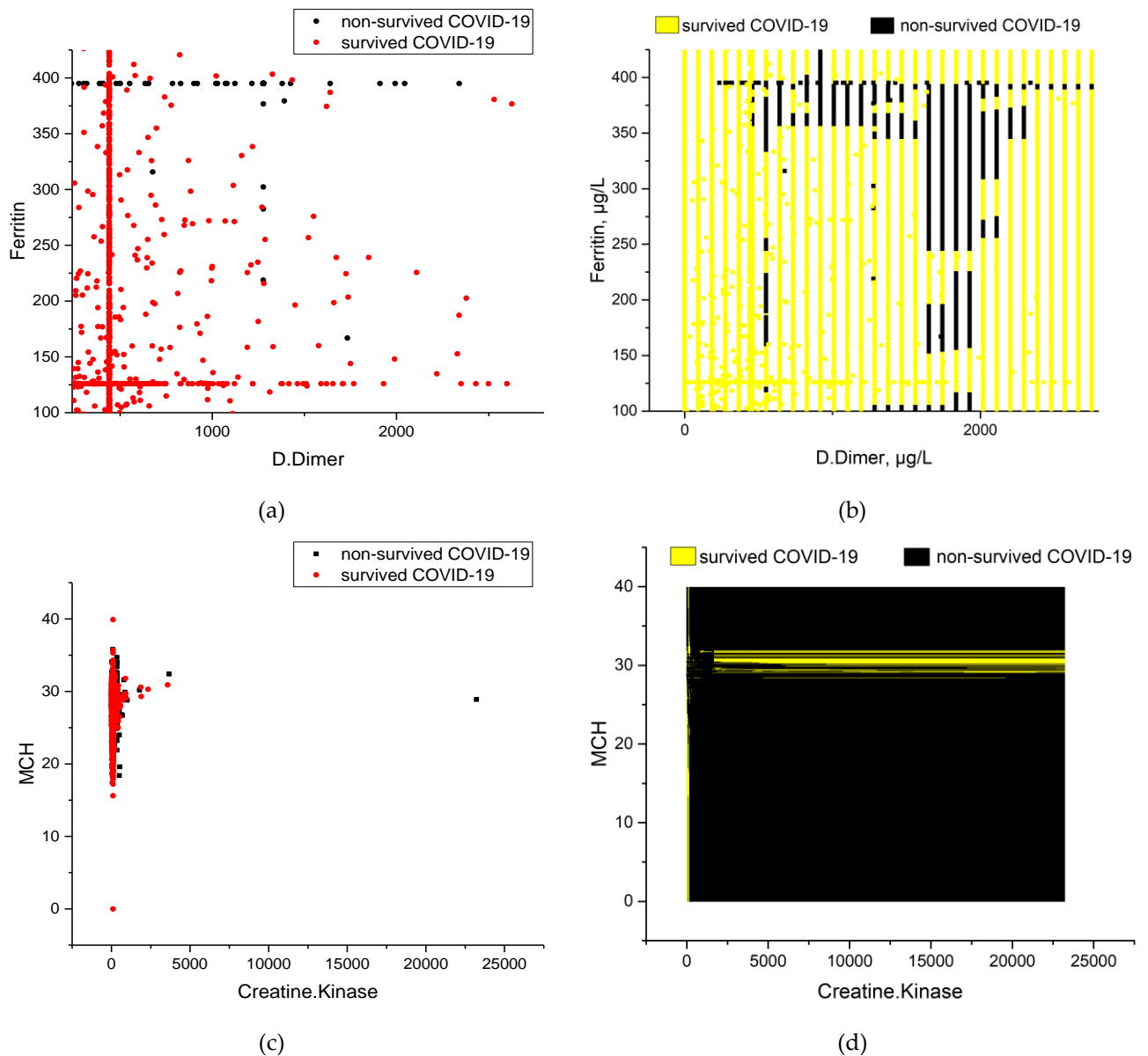


**Figure 13.** a, c) Distributions of non-surviving and surviving COVID-19 patients over the original data on D-dimer-ferritin and CK-MCH feature pairs. c,d) 2D masking technique for patient group classification of the HGB model operated with D-dimer-ferritin and CK-MCH trait pairs.

#### 4. Discussion

COVID-19, caused by the novel coronavirus SARS-Cov-2, is a new disease for humanity and contains many unknowns [16]. During the course of the disease, changes are observed in many biochemical parameters as well as hematological abnormalities [5,12,14,21,22].

While most patients have mild symptoms, some patients may develop severe symptoms such as severe pneumonia, acute respiratory distress syndrome (ARDS), and multiple organ dysfunction syndromes (MODS) [5,22,44]. Therefore, early evaluation of patients who require special care and high mortality expectation and effective identification of relevant biomarkers on large sample groups are important to reduce mortality [5,13,29,35].

In this study, firstly, increasing and decreasing relationship levels between living and deceased patient groups and trait pairs were examined (Table 2). Then, 34 features were determined by statistical approach to determine the most successful ML classifier model

in detecting living and deceased COVID-19 patients (Table 3). Our dataset was balanced with Smoth and our ML models were trained with the balanced dataset, as there was a large sample difference (91% versus 9%) between the groups of patients who lived and died from COVID-19 in our dataset. The patient groups were classified with 16 ML models operated with 34 features, and the most successful was the histogram-based gradient boosting (HGB) model ( $F1^2 = 1$ ) (Table 4). Then, with the HGB model, the most important predictors (12 features) in estimating the mortality of COVID-19 were revealed and lethal risk factors of the disease were determined (Table 5). In addition, pairs of features with the highest classification rate were determined by using binary combinations of all features to determine patient groups (Table 6). Moreover, classification results were found by calculating the most important cut-off values in the classification of patients who lived and died according to one and two threshold values (Table 5 and Table A2-A3).

In this study, patients who died and survived from COVID-19 were highly associated with trait pairs HGB-HCT, RBC-HCT, RBC-HGB, NEU-WBC, INR-PT (Fig 2b,2c). We think that these pairs of features are associated with the prognosis of the disease and have significant negative effects on the immune system during the disease process. Moradi et al. [45] stated that the components of the immune system are the organs most frequently affected by COVID-19 after the lungs, and stated that necrosis and bleeding, as well as spleen atrophy and significant reductions in lymphocyte and neutrophil counts, may occur in these patients. In addition, Guzik et al. [46] noted that these features were highly correlated with the prognosis of the disease. Song et al. [47] determined that increased NEU, WBC, CRP, D-dimer levels may reflect an imbalance in the inflammatory response and these features can be considered as a possible indicator of disease severity in infectious diseases such as sepsis and bacteremia. In one study, it was reported that lower levels of RBC, lymphocytes, platelets, HGB and higher neutrophils were observed in the peripheral blood system of severe COVID-19 patients [48].

In this study, there was a significant decrease in the level of relationship between the patients who died and the pairs of albumin-glucose, ESR-D-dimer, creatinine-ALT, HCT-ESO, ESR-Fibrinogen, and ferritin-D-dimer properties when compared the patients who survived (it was shown as “Down” in Table 2). Here, we can say that the applications applied to the patients who passed away have little effect on the values of these features and that there are hidden relationship structures between these feature pairs and mortality. We think that the decrease in the relationship structure between these trait pairs and the disease increases the mortality. In addition, the relationship rate of all trait pairs shown as “Up” in Table 2 with deceased patients was significantly increased compared to living patients. In particular, the greatly increased level of relationship between NEU-amylase, BASO-CKMB, MPV-AST, D-dimer-creatinine, and MPV-Urea couples and patients who died made us think that important disorders such as kidney and liver functions occur in severe COVID-19 patients. Although the increasing relationship of these trait pairs with the patients who lost their lives points to the lack of self-care, we think that these trait pairs hide important information in increasing the mortality of the disease. It is understood that there are serious increases and decreases in the level of relationship between this feature and its various combinations in the period until death in patients who lost their lives. We think that the difficulties in the management of this process and the serious changes in the levels of these trait pairs indicate very different complications in severe patients. In this context, we can say that the increase or decrease in one of these traits has a significant effect on the metabolism of the other trait, depending on the severity of the disease.

Huyut et al. [12] stated that the patients who died had significant changes in liver and kidney function tests, cardiac troponin and hemogram values, and parameters related to inflammation. They also stated that high ESR, PT, CRP, D-dimer, ferritin and RDW values are the most effective predictors of mortality of COVID-19. Similarly, Chen et al. [49] and Tan et al. [50] determined that disorders resulting from hematological abnormalities were associated with disease severity. Many studies have reported that

leukocytosis and lymphopenia levels are independent predictors of in-hospital mortality [12,44,47]. Huyut et al. [12] did not find EOS and other hematological values to be a predictive risk factor for COVID-19 mortality, while they stated that high NEU, WBC and RDW values are important mortality risk indicators of COVID-19. Similarly, one study noted that neutrophils play an important role in inflammation and this increase contributes to the development of ARDS [51]. In another studies, neutrophil was noted to be an independent predictor of severe disease and associated with hypersensitivity pneumonia in SARS-CoV-2 [51,52]. Although some studies have indicated that increased amylase or lipase indicates a pancreatic injury in COVID-19 patients, this has not been proven in other studies and it has been stated that the increase in these enzymes can also be seen in other clinical conditions [53].

It is known that the use of the F1 score may be more useful than the Accuracy value in cases where the data distributions are not equal. In the classification of surviving patients, all features were found to have a high F1 score for both the original and Smote balanced datasets (Figure 4). In addition, in the classification of patients who died, it was found that the majority of the features had high F1 values for the Smote balanced dataset, while this score was high for only some features for the original dataset (Figure 5).

To select the most important features in defining patient groups, we defined an additional metric ( $F1^2$ ) equal to the product of the F1 metrics of the two classes (Equation 1). We tested the HGB model on the original dataset for single (Fig 6 and Table 5) and dual features (Fig 12 and Table 6), although synthetic data on surviving and deceased patients were well predicted by the model (Supplementary Table A1, Fig 4 and Fig 5). PCT, ferritin, fibrinogen, ESR, PT, and D-dimer were found to be the most important features according to the  $F1^2$  metric for the histogram-based gradient boosting model operated with single features in the classification of surviving and deceased patient groups (Fig 6 and Table 5). In addition, it was observed that PCT and ferritin were the most important feature pairs in the identification of living and deceased patients (precision > 0.98, recall > 0.98,  $F1^2$  > 0.98 in both living and deceased patients) (Table 6 and Fig 12). In addition, other trait pairs run with the HGB model produced an  $F1^2$  value of  $\geq 0.94$  in identifying patient groups (Table 6). Accordingly, our HGB model, which was trained with Smote, was found to largely accurately identify living and deceased COVID-19 patients. In addition, the performance of the HGB model with a single feature ( $F1^2$ ) in the classification of patient groups was found to be more successful than the classification made by considering one and two cut-off values (Figure 11). In addition, the approach of identifying patient groups based on the relationship structure (Spearman) of the characteristics with the patient groups produced the lowest  $F1^2$  results (Figure 11).

In this study, in order to determine the critical risk levels of the features in COVID-19 mortality, the lethal levels of the features were determined with one and two threshold (see section 2.3) value approaches, and patient groups were classified according to these values [Fig 7 ve 8 and Supplementary Table A2 ve A3]. According to the one-threshold approach; PT values greater than 13.50 Sec, D-dimer values greater than 1009.99  $\mu\text{g/L}$  ( $F1^2 = 0.64$ ), INR values greater than 1.51 ( $F1^2 = 0.58$ ), Amylase values greater than 76.79 mg/dL ( $F1^2 = 0.61$ ), and CK-MB values greater than 18.86 u/L were found to be lethal critical levels for COVID-19 mortality. According to the two-threshold approach; It was found that the majority of patients who died had fibrinogen values between 349.98 g/L and 379.05 g/L ( $F1^2 = 0.68$ ), D-dimer values between 1009.99  $\mu\text{g/L}$  ile 10742.71  $\mu\text{g/L}$  ( $F1^2 = 0.65$ ), ESR values between 36.12 ile 56.62 ( $F1^2 = 0.70$ ), ferritin values between 376.2  $\mu\text{g/L}$  ile 396.0  $\mu\text{g/L}$  ( $F1^2 = 0.91$ ), and PCT values between 0.2  $\mu\text{g/L}$  and 5.2  $\mu\text{g/L}$  ( $F1^2 = 0.95$ ). It can be said that the determined value ranges of these features are the most important lethal risk levels. It is noteworthy that procalcitonin and ferritin are the most important feature pairs in the detection of surviving and non-surviving COVID-19 patients, according to both the HGB classifier and the two-threshold approach.

Similar to the findings in this study, many studies have supported the view that any significant increase in PCT levels reflects the development of a critical condition in

COVID-19 [54–58]. Lima et al. [59] stated that due to the characteristic structure of PCT in bacterial and viral infections, it may play a role in the prognosis of COVID-19. Ahmed et al. [54] noted that despite several limitations, elevated PCT levels can be used as a rapid indicator of criticality, worsening clinical picture, and even mortality in COVID-19. Similarly, Lippi et al. [57] stated in a meta-analysis that procalcitonin levels above 0.5 µg/L were correlated with a 5-fold greater risk of serious infection in COVID-19 patients. In another study, Juneja et al. [60] showed that more than 96% of COVID-19 patients with low disease severity had serum procalcitonin levels less than 0.5 µg/L and these patients had better clinical outcomes. Additionally, Juneja et al. noted that PCT levels above 0.5 µg/L are associated with a more serious COVID-19 illness or secondary bacterial infection [60]. A meta-analysis involving Caucasians and South Asians found a strong association between PCT and severity of COVID-19 [54]. This multiethnic assessment further reinforces the importance of PCT as a prognostic biomarker in cases of COVID-19. Lippi et al. [57] emphasizing the properties of PCT, its reliable kinetics, and the potential relationship of its decreasing levels with infection resolution, stated that this feature may be a promising prognostic biomarker in COVID-19. These results support our results in our study.

In a meta-analysis examining a limited number of literature, Henry et al. [61] stated that high hematological findings detected in COVID-19 patients and an increase in values such as D-dimer and IL-6 were accepted as an indicator of widespread cytokine release. Similarly, Onur et al. [16] determined that the increase in biochemical parameters such as ferritin, fibrinogen, D-dimer, and troponin measured at the first hospitalization was associated with mortality. In another studies, Perricone et al. [18] and Torti et al. [62] noted that circulating ferritin levels may not only reflect the acute phase response, but may also play a critical role in inflammation. Also, some studies reported that ferritin as a signaling molecule may be a direct mediator of the immune system [17,63]. Similar to the ferritin findings in this study, Feld et al. [26] and Kernan and Carcillo. [64] stated that ferritin, the essential intracellular iron storage protein, is an acute phase reactant that is elevated in many inflammatory conditions, including acute infections. Onur et al. [16] stated that ferritin, an indicator of systemic inflammation, may be an indicator of disease severity and mortality. Winata and Kurniawan [65] emphasized that D-dimer and fibrinogen degradation product (FDP) are increased in all patients in the late stage of COVID-19. These results suggested that D-Dimer and FDP levels were elevated due to increased hypoxia in severe COVID-19 patients and that these properties were significantly associated with coagulation.

In addition, Huyut et al. [12], Mertoğlu et al. [22] and Huyut and İlkbahar [5] stated that increased fibrinogen, D-dimer, CRP levels cause widespread inflammation and cytokine storm in severe COVID-19 patients, and they stated that high values of these features will increase mortality. In addition, high PT and INR values were interpreted in favor of hypercoagulation in a significant proportion of patients who died in this study. This result supported the idea [12] that the risk of hypercoagulation is high in COVID-19 patients who died. In another study, similar to the findings in this study, increased PT, INR and low aPTT values were interpreted in favor of hypercoagulation in a significant proportion of patients who died [66]. These results contribute to the thought [12,21,22] that cardiovascular pathologies due to coagulation may be increased in patients who died.

## 5. Limitations of the Study

The data set in this article does not include the comorbidities of the patients and the inpatient/outpatient follow-up. However, in practice, it is seen that a training set collected in a certain time period cannot meet all these demands. In addition, this study was carried out only on the Turkish race. Results may need to be tested on other breeds. However, the histogram-based Gradient boosting model approach is easy to retrain and test with data from patients of different races. As more data becomes available, this means that the algorithm will improve in terms of predictive performance of mortality from COVID-19.

## 6. Conclusions

In this study, histogram-based gradient boosting (HGB) model was the most successful ML classifier in detecting surviving and non-surviving COVID-19 patients ( $F1^2 = 1$ ). Major changes were observed in many RBV values of patients who died from COVID-19. This situation indicated that self-care insufficiency developed due to the process in patients who died, but it also suggested that important disorders occurred in the functions of many organs such as liver and kidney. In addition, we can say that an increase or decrease in an RBV value according to the severity of the disease has a significant effect on the metabolism of another RBV value.

The HGB model, which was run with only procalcitonin and ferritin, correctly detected almost all of the COVID-19 patients, both living and deceased (precision > 0.98, recall > 0.98,  $F1^2 > 0.98$ ). In addition, ferritin values between 376.2  $\mu\text{g/L}$  and 396.0  $\mu\text{g/L}$  ( $F1^2 = 0.91$ ) and procalcitonin values between 0.2  $\mu\text{g/L}$  and 5.2  $\mu\text{g/L}$  ( $F1^2 = 0.95$ ) were found to be fatal risk levels for COVID-19.

In this study, we suggest that the HGB model and ferritin and procalcitonin properties can be used to obtain highly successful results in predicting the mortality of COVID-19. In addition, it was found remarkable that procalcitonin and ferritin were the most important features in the determination of patient groups, both by the HGB model and by the two-threshold approach. Accordingly, we think that the critical levels of ferritin and procalcitonin properties we have determined should be taken into account to reduce the lethality of the COVID-19 disease. These biomarkers and its critical levels can also serve as a risk stratification tool for resource allocation and aggressive therapeutics, along with clinical details in over-condensed medical centers in the epidemic.

**Supplementary Materials:** The following supporting information can be downloaded at: [www.mdpi.com/xxx/s1](http://www.mdpi.com/xxx/s1), SARS-CoV-2-RBV3\_Dataset.zip, Readme.pdf. Kindly cite our paper when you wish to use this dataset.

**Author Contributions:** Conceptualization, M.T.H.; methodology, M.T.H., A.V. and M.B.; software, M.T.H., A.V. and M.B.; validation, M.T.H.; formal analysis, M.T.H.; investigation, M.T.H., A.V. and M.B.; resources, M.T.H.; data curation, M.T.H.; writing—original draft preparation, M.T.H., A.V. and M.B.; writing—review and editing, M.T.H., A.V. and M.B.; visualization M.T.H., A.V. and M.B.; supervision, M.T.H.; project administration, M.T.H.; funding acquisition, A.V. All authors have read and agreed to the published version of the manuscript.

**Funding:** This research was supported by the Russian Science Foundation (grant no. 22-11-00055, <https://rscf.ru/en/project/22-11-00055/>).

**Institutional Review Board Statement:** The dataset used in this study was collected in order to be used in various studies in the estimation of the diagnosis, prognosis and mortality of COVID-19. The necessary permissions for the collected dataset were given by the Ministry of Health of the Republic of Turkey and the Ethics Committee of Erzincan Binali Yıldırım University. This study was conducted in accordance with the 1989 Declaration of Helsinki. Erzincan Binali Yıldırım University Human Research Health and Sports Sciences Ethics Committee Decision Number: 2021/02-07.

**Informed Consent Statement:** In this study, a dataset including only routine blood values, RT-PCR results (positive or negative) and treatment units of the patients was downloaded retrospectively from the information system of our hospital in digital environment. A new sample was not taken from the patients. There is no information in the dataset that includes identifying characteristics of individuals. It was stated that routine blood values would only be used in academic studies, and written consent was obtained from the institutions for this. In addition, therefore, written informed consent was not administered for every patient.

**Data Availability Statement:** The data used in this study can be shared with the parties, provided that the article is cited.

**Acknowledgments:** We thank the method of Erzincan Mengücek Gazi Training and Research Hospital for their support in reaching the material used in this study. Special thanks to the editors of the

journal and to the anonymous reviewers for their constructive criticism and improvement suggestions.

**Conflicts of Interest:** The authors declare no conflict of interest.

## Appendix A

**Table A1.** The classification result of SARS-CoV-2-RBV3 datasets for the HGB model using a single input feature for original datasets. Classification metrics (Accuracy(A1), Precision, Recall, F1) separately for classes (survived COVID-19 and non-survived COVID-19).

№	Feature	Precision		Recall		F1		F1 <sup>2</sup>
		surv.	non-surv.	surv.	non-surv.	surv.	non-surv.	
1	ALT	0.8558	0.3245	0.9292	0.1803	0.8909	0.2314	0.20615
2	AST	0.8904	0.3771	0.9369	0.2486	0.913	0.2981	0.27217
3	Albumin	0.6832	0.9341	0.9909	0.2216	0.8086	0.3581	0.28956
4	alkaline.phosphatase	0.8794	0.623	0.9604	0.3331	0.918	0.4324	0.39694
5	Amilase	0.9112	0.9692	0.9968	0.5134	0.952	0.671	0.63879
6	CK.MB	0.8655	0.917	0.9909	0.3975	0.9239	0.554	0.51184
7	Direct_Bilirubin	0.9602	0.5347	0.9554	0.5713	0.9578	0.5503	0.52708
8	Glucose	0.8583	0.535	0.9504	0.267	0.902	0.356	0.32111
9	Creatinine	0.8367	0.6227	0.9583	0.2699	0.8933	0.3763	0.33615
10	Creatine.Kinase	0.8219	0.7678	0.9735	0.2964	0.8911	0.4267	0.38023
11	LDH	0.8498	0.8774	0.9867	0.3659	0.9126	0.5127	0.46789
12	eGFR	0.6849	0.9037	0.9868	0.2174	0.8082	0.3501	0.28295
13	Urea	0.8824	0.7586	0.9743	0.3858	0.926	0.5106	0.47282
14	BASO	0.9953	0.0088	0.9124	0.0786	0.952	0.0157	0.01495
15	ESO	0.9818	0.013	0.9116	0.0533	0.9454	0.0208	0.01966
16	HCT	0.9057	0.0967	0.9123	0.0853	0.9088	0.0887	0.08061
17	HGB	0.9873	0.0264	0.9131	0.1552	0.9488	0.045	0.0427
18	LYM	0.8481	0.1971	0.9165	0.1071	0.8808	0.1382	0.12173
19	MCH	0.9543	0.1097	0.9175	0.1955	0.9355	0.1379	0.12901
20	MCHC	0.9797	0.0439	0.914	0.1375	0.9457	0.0663	0.0627
21	MCV	0.8079	0.2544	0.9182	0.115	0.8594	0.1581	0.13587
22	MONO	0.9061	0.1665	0.9185	0.1491	0.9122	0.1569	0.14312
23	MPV	0.9949	0.0043	0.912	0.1	0.9516	0.0083	0.0079
24	NEU	0.4962	0.6972	0.9442	0.1181	0.6503	0.2019	0.1313
25	PLT	0.8697	0.1671	0.9154	0.1103	0.8918	0.1319	0.11763
26	RBC	0.8837	0.1185	0.9122	0.0888	0.8976	0.1007	0.09039
27	RDW	0.9082	0.2454	0.9258	0.2067	0.9169	0.2241	0.20548
28	WBC	0.9154	0.1798	0.9206	0.1629	0.9178	0.1678	0.15401
29	CRP	0.7386	0.6888	0.961	0.2034	0.835	0.3136	0.26186
30	D.Dimer	0.937	0.842	0.984	0.5677	0.9599	0.6769	0.64976
31	Ferritin	0.9852	0.9253	0.9928	0.8655	0.9889	0.8915	0.8816
32	Fibrinogen	0.9805	0.9562	0.9957	0.8274	0.9881	0.8863	0.87575
33	INR	0.9315	0.847	0.9844	0.548	0.9571	0.663	0.63456
34	PT	0.959	0.8253	0.9828	0.6588	0.9707	0.7312	0.70978
35	Procalcitonin	0.9992	0.9386	0.9941	0.991	0.9966	0.9635	0.96022
36	ESR	0.967	0.8684	0.9871	0.7229	0.9769	0.7868	0.76862
37	Troponin	0.967	0.2898	0.9339	0.4699	0.9501	0.3547	0.337
38	aPTT	0.8837	0.8862	0.9878	0.4266	0.9327	0.5747	0.53602

**Table A2.** Result of classification according to the one-threshold approach of surviving and non-surviving COVID-19 patients for the original dataset.

№	Feature	Type	Vth	Ath	Original base						
					Precision		Recall		F1		F12
					surv.	non-surv.	surv.	non-surv.	surv.	non-surv.	
1	ALT	1	34.84	0.649	0.648	0.665	0.952	0.157	0.771	0.254	0.19583
2	AST	2	33.472	0.806	0.839	0.476	0.942	0.226	0.887	0.306	0.27142
3	Albumin	2	49.08	0.918	0.988	0.206	0.927	0.632	0.956	0.311	0.29732
4	alkaline.phosphatase	2	85.305	0.868	0.893	0.618	0.96	0.362	0.925	0.456	0.4218
5	Amilase	2	76.79	0.936	0.966	0.627	0.963	0.646	0.965	0.636	0.61374
6	CK.MB	2	18.86	0.92	0.935	0.764	0.976	0.538	0.955	0.631	0.6026
7	Direct_Bilirubin	2	0.12985	0.842	0.854	0.725	0.969	0.328	0.908	0.452	0.41042
8	Glucose	2	136.854	0.834	0.862	0.554	0.951	0.283	0.904	0.374	0.3381
9	Creatinine	2	1.16656	0.877	0.918	0.464	0.946	0.358	0.932	0.404	0.37653
10	Creatine.Kinase	2	116.1	0.887	0.912	0.631	0.962	0.414	0.936	0.5	0.468
11	LDH	2	253.26	0.874	0.875	0.867	0.985	0.406	0.927	0.553	0.51263
12	eGFR	1	82.57429	0.77	0.772	0.751	0.969	0.245	0.859	0.369	0.31697
13	Urea	2	39.01	0.818	0.824	0.755	0.972	0.298	0.892	0.427	0.38088
14	BASO	2	0.01026	0.36	0.331	0.657	0.907	0.088	0.485	0.155	0.07517
15	ESO	2	0.01323	0.368	0.344	0.614	0.9	0.084	0.498	0.148	0.0737
16	HCT	1	44.0946	0.261	0.203	0.854	0.934	0.096	0.334	0.172	0.05745
17	HGB	1	15.3972	0.229	0.162	0.906	0.946	0.096	0.277	0.174	0.0482
18	LYM	1	1.72672	0.414	0.384	0.712	0.931	0.102	0.544	0.179	0.09738
19	MCH	2	29.6058	0.721	0.761	0.318	0.919	0.116	0.832	0.17	0.14144
20	MCHC	1	33.696	0.56	0.56	0.558	0.928	0.111	0.699	0.185	0.12931
21	MCV	2	83.7456	0.503	0.489	0.639	0.932	0.11	0.642	0.187	0.12005
22	MONO	2	0.45078	0.422	0.392	0.73	0.936	0.106	0.553	0.185	0.10231
23	MPV	1	11.0988	0.265	0.214	0.785	0.91	0.09	0.346	0.161	0.05571
24	NEU	2	4.379	0.571	0.56	0.691	0.948	0.134	0.704	0.224	0.1577
25	PLT	1	245.85	0.451	0.423	0.73	0.941	0.111	0.584	0.193	0.11271
26	RBC	1	5.06844	0.34	0.294	0.803	0.938	0.101	0.448	0.179	0.08019
27	RDW	2	13.2096	0.598	0.585	0.73	0.956	0.148	0.726	0.246	0.1786
28	WBC	2	6.2006	0.492	0.468	0.738	0.948	0.12	0.626	0.207	0.12958
29	CRP	2	19.488	0.72	0.719	0.738	0.965	0.205	0.824	0.321	0.2645
30	D.Dimer	2	1009.998	0.92	0.922	0.906	0.99	0.533	0.955	0.671	0.6408
31	Ferritin	2	376.2	0.878	0.871	0.94	0.993	0.419	0.928	0.579	0.53731
32	Fibrinogen	2	349.98608	0.834	0.82	0.979	0.997	0.349	0.9	0.515	0.4635
33	INR	2	1.15151	0.909	0.918	0.811	0.98	0.495	0.948	0.615	0.58302
34	PT	2	13.50512	0.901	0.903	0.88	0.987	0.471	0.943	0.614	0.579
35	Procalcitonin	2	0.2	0.882	0.878	0.923	0.991	0.427	0.931	0.583	0.54277
36	ESR	2	36.125	0.883	0.88	0.918	0.991	0.43	0.932	0.585	0.54522
37	Troponin	2	13.2	0.906	0.968	0.279	0.932	0.461	0.949	0.348	0.33025
38	aPTT	1	32.4594	0.875	0.87	0.931	0.992	0.413	0.927	0.573	0.53117

**Table A3.** Result of classification according to the two-threshold approach of surviving and non-surviving COVID-19 patients for the original dataset.

№	Feature	Type	$V_{th_1}$	$V_{th_2}$	$A_{th}$	Original base						
						Precision		Recall		F1		F1 <sup>2</sup>
						surv.	non-surv.	surv.	non-surv.	surv.	non-surv.	
1	ALT	1	34.84	35.36	0.518	0.483	0.876	0.975	0.143	0.646	0.246	0.15892
2	AST	1	32.949	33.472	0.536	0.492	0.979	0.996	0.16	0.659	0.275	0.18123
3	Albumin	1	36.81	49.08	0.808	0.826	0.627	0.957	0.262	0.887	0.37	0.32819
4	alkaline.phos- phatase	1	83.582	85.305	0.725	0.701	0.97	0.996	0.242	0.823	0.388	0.31932
5	Amilase	1	72.92	76.79	0.922	0.917	0.974	0.997	0.535	0.955	0.691	0.6599
6	CK.MB	1	18.4	18.86	0.832	0.816	0.996	0.999	0.347	0.898	0.515	0.46247
7	Direct_Bilirubin	1	0.04995	0.12985	0.836	0.845	0.747	0.971	0.322	0.904	0.45	0.4068
8	Glucose	1	135.631	136.854	0.557	0.514	0.991	0.998	0.167	0.679	0.286	0.19419
9	Creatinine	1	0.96492	1.16656	0.617	0.595	0.845	0.975	0.171	0.739	0.284	0.20988
10	Creatine.Kinase	1	92.88	116.1	0.663	0.636	0.931	0.989	0.201	0.774	0.331	0.25619
11	LDH	2	253.26	597.64	0.876	0.877	0.867	0.985	0.411	0.928	0.557	0.5169
12	eGFR	1	82.5742	146.2250	0.77	0.772	0.755	0.97	0.246	0.859	0.371	0.31869
13	Urea	1	0	39.01	0.818	0.824	0.755	0.972	0.298	0.892	0.427	0.38088
14	BASO	1	0.00988	0.01026	0.322	0.277	0.777	0.926	0.096	0.426	0.17	0.07242
15	ESO	2	0.01323	0.11907	0.574	0.596	0.352	0.903	0.079	0.718	0.129	0.09262
16	HCT	2	30.1257	44.0946	0.293	0.246	0.768	0.915	0.091	0.388	0.163	0.06324
17	HGB	2	9.5128	15.3972	0.252	0.193	0.85	0.929	0.094	0.319	0.169	0.05391
18	LYM	2	0.59356	1.72672	0.481	0.466	0.635	0.928	0.105	0.62	0.18	0.1116
19	MCH	2	29.6058	35.6706	0.722	0.762	0.313	0.918	0.115	0.833	0.168	0.13994
20	MCHC	2	28.431	33.696	0.562	0.563	0.558	0.928	0.112	0.701	0.186	0.13039
21	MCV	2	83.7456	113.0624	0.503	0.489	0.639	0.932	0.11	0.642	0.188	0.1207
22	MONO	2	0.45078	6.70023	0.423	0.393	0.73	0.936	0.106	0.554	0.185	0.10249
23	MPV	2	9.9018	11.0988	0.539	0.549	0.438	0.908	0.087	0.685	0.146	0.10001
24	NEU	2	4.379	24.853	0.573	0.561	0.691	0.948	0.134	0.705	0.225	0.15862
25	PLT	2	108.025	245.85	0.474	0.453	0.687	0.936	0.11	0.611	0.19	0.11609
26	RBC	2	0.00722	5.06844	0.34	0.295	0.803	0.938	0.101	0.449	0.179	0.08037
27	RDW	2	13.2096	21.1712	0.603	0.592	0.717	0.955	0.148	0.731	0.245	0.1791
28	WBC	2	6.2006	44.054	0.493	0.469	0.738	0.948	0.12	0.627	0.207	0.12979
29	CRP	2	19.488	252.938	0.722	0.721	0.73	0.964	0.205	0.825	0.32	0.264
30	D.Dimer	2	1009.99	10742.70	0.923	0.925	0.906	0.99	0.544	0.956	0.68	0.65008
31	Ferritin	2	376.2	396	0.984	0.989	0.931	0.993	0.897	0.991	0.914	0.90577
32	Fibrinogen	2	349.986	379.054	0.927	0.923	0.97	0.997	0.553	0.958	0.704	0.67443
33	INR	2	1.15151	10.4753	0.91	0.92	0.811	0.98	0.5	0.949	0.619	0.58743
34	PT	2	13.5051	110.0950	0.902	0.904	0.88	0.987	0.475	0.944	0.617	0.58245
35	Procalcitonin	2	0.2	5.2	0.992	1	0.918	0.992	0.995	0.996	0.955	0.95118
36	ESR	2	36.125	56.625	0.939	0.944	0.888	0.988	0.609	0.966	0.723	0.69842
37	Troponin	2	13.2	3269.2	0.906	0.969	0.275	0.931	0.464	0.95	0.345	0.32775
38	aPTT	2	22.1582	32.4594	0.878	0.873	0.927	0.992	0.419	0.929	0.577	0.53603

## References

1. Huyut, M.T.; Soygüder, S. The Multi-Relationship Structure between Some Symptoms and Features Seen during

- the New Coronavirus 19 Infection and the Levels of Anxiety and Depression Post-Covid. *East. J. Med.* **2022**, *27*, 1–10, doi:10.5505/ejm.2022.35336.
2. Huyut, M.T.; Kocaturk, İ. The Effect of Some Symptoms and Features During the Infection Period on the Level of Anxiety and Depression of Adults After Recovery From COVID-19. *Curr. Psychiatry Res. Rev.* **2022**, *18*, doi:10.2174/2666082218666220325105504.
  3. Feigin, E.; Levinson, T.; Wasserman, A.; Shenhar-Tsarfaty, S.; Berliner, S.; Ziv-Baran, T. Age-Dependent Biomarkers for Prediction of In-Hospital Mortality in COVID-19 Patients. *J. Clin. Med.* **2022**, *11*, doi:10.3390/jcm11102682.
  4. Huyut, M.T. Automatic Detection of Severely and Mildly Infected COVID-19 Patients with Supervised Machine Learning Models. *IRBM* **2022**, *1*, 1–12, doi:10.1016/j.irbm.2022.05.006.
  5. Huyut, M.T.; İlkbahar, F. The Effectiveness of Blood Routine Parameters and Some Biomarkers as a Potential Diagnostic Tool in the Diagnosis and Prognosis of Covid-19 Disease. *Int. Immunopharmacol.* **2021**, *98*, doi:10.1016/j.intimp.2021.107838.
  6. Ciotti, M.; Angeletti, S.; Minieri, M.; Giovannetti, M.; Benvenuto, D.; Pascarella, S.; Sagnelli, C.; Bianchi, M.; Bernardini, S.; Ciccozzi, M. COVID-19 Outbreak: An Overview. *Chemotherapy* **2020**, *64*, 215–223, doi:10.1159/000507423.
  7. Richardson, S.; Hirsch, J.S.; Narasimhan, M.; Crawford, J.M.; McGinn, T.; Davidson, K.W.; Barnaby, D.P.; Becker, L.B.; Chelico, J.D.; Cohen, S.L.; et al. Presenting Characteristics, Comorbidities, and Outcomes among 5700 Patients Hospitalized with COVID-19 in the New York City Area. *JAMA - J. Am. Med. Assoc.* **2020**, *323*, 2052–2059, doi:10.1001/jama.2020.6775.
  8. Asch, D.A.; Sheils, N.E.; Islam, M.N.; Chen, Y.; Werner, R.M.; Buresh, J.; Doshi, J.A. Variation in US Hospital Mortality Rates for Patients Admitted with COVID-19 during the First 6 Months of the Pandemic. *JAMA Intern. Med.* **2021**, *181*, 471–478, doi:10.1001/jamainternmed.2020.8193.
  9. Strålin, K.; Wahlström, E.; Walther, S.; Bennet-Bark, A.M.; Heurgren, M.; Lindén, T.; Holm, J.; Hanberger, H. Mortality Trends among Hospitalised COVID-19 Patients in Sweden: A Nationwide Observational Cohort Study. *Lancet Reg. Heal. - Eur.* **2021**, *4*, doi:10.1016/j.lanepe.2021.100054.
  10. Strålin, K.; Wahlström, E.; Walther, S.; Bennet-Bark, A.M.; Heurgren, M.; Lindén, T.; Holm, J.; Hanberger, H. Mortality in Hospitalized COVID-19 Patients Was Associated with the COVID-19 Admission Rate during the First Year of the Pandemic in Sweden. *Infect. Dis. (Auckl).* **2022**, *54*, 145–151, doi:10.1080/23744235.2021.1983643.
  11. Zheng, Y.; Zhang, Y.; Chi, H.; Chen, S.; Peng, M.; Luo, L.; Chen, L.; Li, J.; Shen, B.; Wang, D. The Hemocyte Counts as a Potential Biomarker for Predicting Disease Progression in COVID-19: A Retrospective Study. *Clin. Chem. Lab. Med.* **2020**, *58*, 1106–1115, doi:10.1515/cclm-2020-0377.
  12. Tahir Huyut, M.; Huyut, Z.; İlkbahar, F.; Mertoğlu, C. What Is the Impact and Efficacy of Routine Immunological, Biochemical and Hematological Biomarkers as Predictors of COVID-19 Mortality? *Int. Immunopharmacol.* **2022**,

105, doi:10.1016/j.intimp.2022.108542.

13. Huyut, M.; Üstündağ, H. Prediction of Diagnosis and Prognosis of COVID-19 Disease by Blood Gas Parameters Using Decision Trees Machine Learning Model: A Retrospective Observational Study. *Med. Gas Res.* **2022**, *12*, 60–66, doi:10.4103/2045-9912.326002.
14. HUYUT, M.T.; HUYUT, Z. Forecasting of Oxidant/Antioxidant Levels of COVID-19 Patients by Using Expert Models with Biomarkers Used in the Diagnosis/Prognosis of COVID-19. *Int. Immunopharmacol.* **2021**, *100*, doi:10.1016/j.intimp.2021.108127.
15. Zhou, C.; Chen, Y.; Ji, Y.; He, X.; Xue, D. Increased Serum Levels of Hepcidin and Ferritin Are Associated with Severity of COVID-19. *Med. Sci. Monit.* **2020**, *26*, 1–6, doi:10.12659/MSM.926178.
16. Tural Onur, S.; Altın, S.; Sokucu, S.N.; Fikri, B.İ.; Barça, T.; Bolat, E.; Toptaş, M. Could Ferritin Level Be an Indicator of COVID-19 Disease Mortality? *J. Med. Virol.* **2021**, *93*, 1672–1677, doi:10.1002/jmv.26543.
17. Gómez-Pastora, J.; Weigand, M.; Kim, J.; Wu, X.; Strayer, J.; Palmer, A.F.; Zborowski, M.; Yazer, M.; Chalmers, J.J. Hyperferritinemia in Critically Ill COVID-19 Patients – Is Ferritin the Product of Inflammation or a Pathogenic Mediator? *Clin. Chim. Acta* **2020**, *509*, 249–251, doi:10.1016/j.cca.2020.06.033.
18. Perricone, C.; Bartoloni, E.; Bursi, R.; Cafaro, G.; Guidelli, G.M.; Shoenfeld, Y.; Gerli, R. COVID-19 as Part of the Hyperferritinemic Syndromes: The Role of Iron Depletion Therapy. *Immunol. Res.* **2020**, *68*, 213–224, doi:10.1007/s12026-020-09145-5.
19. Luo, X.; Zhou, W.; Yan, X.; Guo, T.; Wang, B.; Xia, H.; Ye, L.; Xiong, J.; Jiang, Z.; Liu, Y.; et al. Prognostic Value of C-Reactive Protein in Patients with Coronavirus 2019. *Clin. Infect. Dis.* **2020**, *71*, 2174–2179, doi:10.1093/cid/ciaa641.
20. Cecconi, M.; Piovani, D.; Brunetta, E.; Aghemo, A.; Greco, M.; Ciccarelli, M.; Angelini, C.; Voza, A.; Omodei, P.; Vespa, E.; et al. Early Predictors of Clinical Deterioration in a Cohort of 239 Patients Hospitalized for Covid-19 Infection in Lombardy, Italy. *J. Clin. Med.* **2020**, *9*, 1–16, doi:10.3390/jcm9051548.
21. Mertoglu, C.; Huyut, M.T.; Arslan, Y.; Ceylan, Y.; Coban, T.A. How Do Routine Laboratory Tests Change in Coronavirus Disease 2019? *Scand. J. Clin. Lab. Invest.* **2021**, *81*, 24–33, doi:10.1080/00365513.2020.1855470.
22. Mertoglu, C.; Huyut, M.; Olmez, H.; Tosun, M.; Kantarci, M.; Coban, T. COVID-19 Is More Dangerous for Older People and Its Severity Is Increasing: A Case-Control Study. *Med. Gas Res.* **2022**, *12*, 51–54, doi:10.4103/2045-9912.325992.
23. Huyut, M.T.; Velichko, A. Diagnosis and Prognosis of COVID-19 Disease Using Routine Blood Values and LogNNet Neural Network. *Sensors* **2022**, *22*, 4820, doi:10.3390/s22134820.
24. Zhang, J. jin; Cao, Y. yuan; Tan, G.; Dong, X.; Wang, B. chen; Lin, J.; Yan, Y. qin; Liu, G. hui; Akdis, M.; Akdis, C.A.; et al. Clinical, Radiological, and Laboratory Characteristics and Risk Factors for Severity and Mortality of 289 Hospitalized COVID-19 Patients. *Allergy Eur. J. Allergy Clin. Immunol.* **2021**, *76*, 533–550, doi:10.1111/all.14496.

- 
25. Ponti, G.; Maccaferri, M.; Ruini, C.; Tomasi, A.; Ozben, T. Biomarkers Associated with COVID-19 Disease Progression. *Crit. Rev. Clin. Lab. Sci.* **2020**, *57*, 389–399, doi:10.1080/10408363.2020.1770685.
  26. Feld, J.; Tremblay, D.; Thibaud, S.; Kessler, A.; Naymagon, L. Ferritin Levels in Patients with COVID-19: A Poor Predictor of Mortality and Hemophagocytic Lymphohistiocytosis. *Int. J. Lab. Hematol.* **2020**, *42*, 773–779, doi:10.1111/ijlh.13309.
  27. Hou, H.; Zhang, B.; Huang, H.; Luo, Y.; Wu, S.; Tang, G.; Liu, W.; Mao, L.; Mao, L.; Wang, F.; et al. Using IL-2R/Lymphocytes for Predicting the Clinical Progression of Patients with COVID-19. *Clin. Exp. Immunol.* **2020**, *201*, 76–84, doi:10.1111/cei.13450.
  28. Ji, D.; Ji, D.; Zhang, D.; Chen, Z.; Xu, Z.; Zhao, P.; Zhang, M.; Zhang, L.; Cheng, G.; Wang, Y.; et al. SSRN-Id3539674.
  29. Cheng, L.; Li, H.; Li, L.; Liu, C.; Yan, S.; Chen, H.; Li, Y. Ferritin in the Coronavirus Disease 2019 (COVID-19): A Systematic Review and Meta-Analysis. *J. Clin. Lab. Anal.* **2020**, *34*, 1–18, doi:10.1002/jcla.23618.
  30. Kukar, M.; Gunčar, G.; Vovko, T.; Podnar, S.; Černelč, P.; Brvar, M.; Zalaznik, M.; Notar, M.; Moškon, S.; Notar, M. COVID-19 Diagnosis by Routine Blood Tests Using Machine Learning. *Sci. Rep.* **2021**, *11*, 10738, doi:10.1038/s41598-021-90265-9.
  31. Podnar, S.; Kukar, M.; Gunčar, G.; Notar, M.; Gošnjak, N.; Notar, M. Diagnosing Brain Tumours by Routine Blood Tests Using Machine Learning. *Sci. Rep.* **2019**, *9*, 1–7, doi:10.1038/s41598-019-51147-3.
  32. Velichko, A.; Huyut, M.T.; Belyaev, M.; Izotov, Y.; Korzun, D. Machine Learning Sensors for Diagnosis of COVID-19 Disease Using Routine Blood Values for Internet of Things Application. *Sensors* **2022**, *22*.
  33. Booth, A.L.; Abels, E.; McCaffrey, P. Development of a Prognostic Model for Mortality in COVID-19 Infection Using Machine Learning. *Mod. Pathol.* **2021**, *34*, 522–531, doi:10.1038/s41379-020-00700-x.
  34. Luo, Y.; Szolovits, P.; Dighe, A.S.; Baron, J.M. Using Machine Learning to Predict Laboratory Test Results. *Am. J. Clin. Pathol.* **2016**, *145*, 778–788, doi:10.1093/ajcp/aqw064.
  35. Doğanay, F.; Elkonca, F.; Seyhan, A.U.; Yılmaz, E.; Batirel, A.; Ak, R. Shock Index as a Predictor of Mortality among the Covid-19 Patients. *Am. J. Emerg. Med.* **2021**, *40*, 106–109, doi:10.1016/j.ajem.2020.12.053.
  36. Zhang, S.; Huang, S.; Liu, J.; Dong, X.; Meng, M.; Chen, L.; Wen, Z.; Zhang, L.; Chen, Y.; Du, H.; et al. Since January 2020 Elsevier Has Created a COVID-19 Resource Centre with Free Information in English and Mandarin on the Novel Coronavirus COVID- 19 . The COVID-19 Resource Centre Is Hosted on Elsevier Connect , the Company ' s Public News and Information . **2020**.
  37. Formica, V.; Minieri, M.; Bernardini, S.; Ciotti, M.; D'Agostini, C.; Roselli, M.; Andreoni, M.; Morelli, C.; Parisi, G.; Federici, M.; et al. Complete Blood Count Might Help to Identify Subjects with High Probability of Testing Positive to SARS-CoV-2. *Clin. Med. J. R. Coll. Physicians London* **2020**, *20*, 114–119, doi:10.7861/CLINMED.2020-0373.

- 
38. Banerjee, A.; Ray, S.; Vorselaars, B.; Kitson, J.; Mamalakis, M.; Weeks, S.; Baker, M.; Mackenzie, L.S. Use of Machine Learning and Artificial Intelligence to Predict SARS-CoV-2 Infection from Full Blood Counts in a Population. *Int. Immunopharmacol.* **2020**, *86*, doi:10.1016/j.INTIMP.2020.106705.
39. Avila, E.; Kahmann, A.; Alho, C.; Dorn, M. Hemogram Data as a Tool for Decision-Making in COVID-19 Management: Applications to Resource Scarcity Scenarios. *PeerJ* **2020**, *2020*, doi:10.7717/peerj.9482.
40. Joshi, R.P.; Pejaver, V.; Hammarlund, N.E.; Sung, H.; Kyu, S.; Lee, H.; Scott, G.; Gombar, S.; Shah, N.; Mooney, S.; et al. Since January 2020 Elsevier Has Created a COVID-19 Resource Centre with Free Information in English and Mandarin on the Novel Coronavirus COVID-19. The COVID-19 Resource Centre Is Hosted on Elsevier Connect, the Company's Public News and Information. **2020**.
41. Zhu, J.S.; Ge, P.; Jiang, C.; Zhang, Y.; Li, X.; Zhao, Z.; Zhang, L.; Duong, T.Q. Deep-learning Artificial Intelligence Analysis of Clinical Variables Predicts Mortality in COVID-19 Patients. *J. Am. Coll. Emerg. Physicians Open* **2020**, *1*, 1364–1373, doi:10.1002/emp2.12205.
42. Soltan, A.A.; Kouchaki, S.; Zhu, T.; Kiyasseh, D.; Taylor, T.; Hussain, Z.B.; Peto, T.; Brent, A.J.; Eyre, D.W.; Clifton, D. Artificial Intelligence Driven Assessment of Routinely Collected Healthcare Data Is an Effective Screening Test for COVID-19 in Patients Presenting to Hospital. *medRxiv* **2020**, 2020.07.07.20148361.
43. Soares, F. A Novel Specific Artificial Intelligence-Based Method to Identify COVID-19 Cases Using Simple Blood Exams. *medRxiv* **2020**, 2020.04.10.20061036.
44. Lippi, G.; Plebani, M.; Henry, B.M. Thrombocytopenia Is Associated with Severe Coronavirus Disease 2019 (COVID-19) Infections: A Meta-Analysis. *Clin. Chim. Acta* **2020**, *506*, 145–148, doi:10.1016/j.cca.2020.03.022.
45. Vafadar Moradi, E.; Teimouri, A.; Rezaee, R.; Morovatdar, N.; Foroughian, M.; Layegh, P.; Rezvani Kakhki, B.; Ahmadi Koupaee, S.R.; Ghorani, V. Increased Age, Neutrophil-to-Lymphocyte Ratio (NLR) and White Blood Cells Count Are Associated with Higher COVID-19 Mortality. *Am. J. Emerg. Med.* **2021**, *40*, 11–14, doi:10.1016/j.ajem.2020.12.003.
46. Guzik, T.J.; Mohiddin, S.A.; Dimarco, A.; Patel, V.; Savvatis, K.; Marelli-Berg, F.M.; Madhur, M.S.; Tomaszewski, M.; Maffia, P.; D'Acquisto, F.; et al. COVID-19 and the Cardiovascular System: Implications for Risk Assessment, Diagnosis, and Treatment Options. *Cardiovasc. Res.* **2020**, *116*, 1666–1687, doi:10.1093/cvr/cvaa106.
47. Song, H.; Kim, H.J.; Park, K.N.; Kim, S.H.; Oh, S.H.; Youn, C.S. Neutrophil to Lymphocyte Ratio Is Associated with In-Hospital Mortality in Older Adults Admitted to the Emergency Department. *Am. J. Emerg. Med.* **2021**, *40*, 133–137, doi:10.1016/j.ajem.2020.01.044.
48. Mo, P.; Xing, Y.; Xiao, Y.; Deng, L.; Zhao, Q.; Wang, H.; Xiong, Y.; Cheng, Z.; Gao, S.; Liang, K.; et al. Clinical Characteristics of Refractory Coronavirus Disease 2019 in Wuhan, China. *Clin. Infect. Dis.* **2021**, *73*, E4208–E4213, doi:10.1093/cid/ciaa270.
49. Chen, N.; Zhou, M.; Dong, X.; Qu, J.; Gong, F.; Han, Y.; Qiu, Y.; Wang, J.; Liu, Y.; Wei, Y.; et al. Epidemiological and Clinical Characteristics of 99 Cases of 2019 Novel Coronavirus Pneumonia in Wuhan, China: A Descriptive

- Study. *Lancet* **2020**, *395*, 507–513, doi:10.1016/S0140-6736(20)30211-7.
50. Tan, L.; Wang, Q.; Zhang, D.; Ding, J.; Huang, Q.; Tang, Y.Q.; Wang, Q.; Miao, H. Lymphopenia Predicts Disease Severity of COVID-19: A Descriptive and Predictive Study. *Signal Transduct. Target. Ther.* **2020**, *5*, 16–18, doi:10.1038/s41392-020-0148-4.
  51. Wu, C.; Chen, X.; Cai, Y.; Xia, J.; Zhou, X.; Xu, S.; Huang, H.; Zhang, L.; Zhou, X.; Du, C.; et al. Risk Factors Associated with Acute Respiratory Distress Syndrome and Death in Patients with Coronavirus Disease 2019 Pneumonia in Wuhan, China. *JAMA Intern. Med.* **2020**, *180*, 934–943, doi:10.1001/jamainternmed.2020.0994.
  52. Zhu, N.; Zhang, D.; Wang, W.; Li, X.; Yang, B.; Song, J.; Zhao, X.; Huang, B.; Shi, W.; Lu, R.; et al. A Novel Coronavirus from Patients with Pneumonia in China, 2019. *N. Engl. J. Med.* **2020**, *382*, 727–733.
  53. Pribadi, R.R.; Simadibrata, M. Increased Serum Amylase and/or Lipase in Coronavirus Disease 2019 (COVID-19) Patients: Is It Really Pancreatic Injury? *JGH Open* **2021**, *5*, 190–192, doi:10.1002/jgh3.12436.
  54. Ahmed, S.; Jafri, L.; Hoodbhoy, Z.; Siddiqui, I. Prognostic Value of Serum Procalcitonin in Covid-19 Patients: A Systematic Review. *Indian J. Crit. Care Med.* **2021**, *25*, 77–84, doi:10.5005/jp-journals-10071-23706.
  55. Li, X.; Wang, L.; Yan, S.; Yang, F.; Xiang, L.; Zhu, J.; Shen, B.; Gong, Z. Clinical Characteristics of 25 Death Cases with COVID-19: A Retrospective Review of Medical Records in a Single Medical Center, Wuhan, China. *Int. J. Infect. Dis.* **2020**, *94*, 128–132, doi:10.1016/j.ijid.2020.03.053.
  56. Ke, C.; Wang, Y.; Zeng, X.; Yang, C.; Hu, Z. 2019 Novel Coronavirus Disease (COVID-19) in Hemodialysis Patients: A Report of Two Cases. *Clin. Biochem.* **2020**, *81*, 9–12, doi:10.1016/j.clinbiochem.2020.04.008.
  57. Lippi, G.; Plebani, M. Procalcitonin in Patients with Severe Coronavirus Disease 2019 (COVID-19): A Meta-Analysis. *Clin. Chim. Acta* **2020**, *505*, 190–191, doi:10.1016/j.cca.2020.03.004.
  58. Lin, L.; Lu, L.; Cao, W.; Li, T. Hypothesis for Potential Pathogenesis of SARS-CoV-2 Infection—a Review of Immune Changes in Patients with Viral Pneumonia. *Emerg. Microbes Infect.* **2020**, *9*, 727–732, doi:10.1080/22221751.2020.1746199.
  59. Lima, M.E. de S.; Barros, L.C.M.; Aragão, G.F. Could Autism Spectrum Disorders Be a Risk Factor for COVID-19? *Med. Hypotheses* **2020**, *144*, 109899, doi:10.1016/j.mehy.2020.109899.
  60. Juneja, D.; Savio, R.D.; Srinivasan, S.; Pandit, R.A.; Ramasubban, S.; Reddy, P.K.; Singh, M.; Gopal, P.B.N.; Chaudhry, D.; Govil, D.; et al. Basic Critical Care for Management of COVID-19 Patients: Position Paper of Indian Society of Critical Care Medicine, Part-I. *Indian J. Crit. Care Med.* **2020**, *24*, S244–S253, doi:10.5005/jp-journals-10071-23601.
  61. Henry, B.M.; De Oliveira, M.H.S.; Benoit, S.; Plebani, M.; Lippi, G. Hematologic, Biochemical and Immune Biomarker Abnormalities Associated with Severe Illness and Mortality in Coronavirus Disease 2019 (COVID-19): A Meta-Analysis. *Clin. Chem. Lab. Med.* **2020**, *58*, 1021–1028, doi:10.1515/cclm-2020-0369.
  62. Torti, F.M.; Torti, S. V. Regulation of Ferritin Genes and Protein. *Blood* **2002**, *99*, 3505–3516,

---

doi:10.1182/blood.V99.10.3505.

63. Rosário, C.; Zandman-Goddard, G.; Meyron-Holtz, E.G.; D’Cruz, D.P.; Shoenfeld, Y. The Hyperferritinemic Syndrome: Macrophage Activation Syndrome, Still’s Disease, Septic Shock and Catastrophic Antiphospholipid Syndrome. *BMC Med.* **2013**, *11*, doi:10.1186/1741-7015-11-185.
64. Kernan, K.F.; Carcillo, J.A. Hyperferritinemia and Inflammation. *Int. Immunol.* **2017**, *29*, 401–409, doi:10.1093/intimm/dxx031.
65. Winata, S.; Kurniawan, A. Coagulopathy in COVID-19: A Systematic Review. *Medicus* **2021**, *8*, 72, doi:10.19166/med.v8i2.3444.
66. Amgalan, A.; Othman, M. Hemostatic Laboratory Derangements in COVID-19 with a Focus on Platelet Count. **2020**, doi:10.1080/09537104.2020.1768523.